arXiv:astro-ph/0009165v1 11 Sep 2000

Inhomogeneous Chemical Evolution of the Galactic Halo: Abundance of r-process Elements

Claudia Travaglio[1,2], Daniele Galli[3], Andreas Burkert[1]

1. Max-Planck Institut für Astronomie, Königstuhl, 17, 69117 Heidelberg, Germany
2. Dipartimento di Astronomia e Scienza dello Spazio, Largo E. Fermi 5, I-50125 Firenze, Italy
3. Osservatorio Astrofisico di Arcetri, Largo E. Fermi 5, I-50125 Firenze, Italy

ABSTRACT

We present a stochastic model based on the Monte Carlo technique to study the inhomogeneous chemical evolution of the Galactic halo. In particular, we consider the local enrichment and subsequent mixing of the interstellar gas resulting from bursts of star formation, following explicitly the fragmentation and coalescence of interstellar gas clouds. The model takes into account the mixing of halo gas through cloud-cloud collisions and the delayed mixing of supernova ejecta into the interstellar medium. The consequences of the infall of halo gas onto the Galactic disk are also discussed. The mass spectrum of clouds, the age-metallicity relation, and the G-dwarf distribution are investigated at different times. We analyze in detail the predictions of our model for the abundance of elements like Eu, Ba, and Sr in the Galactic halo, following their production by r-process nucleosynthesis for different assumptions on the supernova mass range. Finally, we compare our results with spectroscopic data for the chemical composition of metal-poor halo stars.

Subject headings: Galaxy: halo, evolution, abundances - ISM: clouds, kinematics and dynamics

1. Introduction

The enrichment of the interstellar medium (hereafter ISM) in heavy elements by successive generations of stars is a key issue in understanding the chemical evolution of galaxies in general, and the formation history and abundance distribution of stellar populations in our Galaxy in particular. From an observational point of view, very metal poor stars provide

important clues to reconstruct the chemo-dynamical aspects of the first stages of halo evolution. Therefore, a large body of spectroscopic abundance determinations has been obtained for halo stars. In particular, observational studies related to the heavy element abundances in the Galactic halo have shown that stars of similar metallicity exhibit large abundance variations, over about 2 dex in [element/Fe], for heavy elements like Eu, Ba and Sr (see e.g. Gilroy et al. 1988, Ryan & Norris 1991, Gratton & Sneden 1994, McWilliam et al. 1995b, Ryan, Norris & Beers 1996, and, more recently, McWilliam 1998, Sneden et al. 1998, Burris et al. 2000). However, the actual nature of this scatter, and the possible influence of various effects like different calibration methods or data reduction procedures, is still unclear. If the observed scatter is *intrinsic*, one is led to consider a scenario in which the oldest halo stars were formed out of gas of strongly inhomogeneous chemical composition. For instance, the peculiar abundances determined by Sneden et al. (1994) and McWilliam et al. (1995a) in the star CS 22892-052 (where r-process elements are enhanced over about 40 times the solar value) provide support to this hypothesis. Similar studies of objects in the Magellanic clouds (e.g. Cohen 1982, Da Costa 1991, Olsewski et al. 1991) and dwarf galaxies (e.g. Pilyugin 1992, Kunth et al. 1994) suggest that inhomogeneous chemical evolution is a common phenomenon in nearby galaxies as well.

From a theoretical point of view, as first suggested by Truran (1981), the presence of r-process elements in low metallicity halo stars is indicative of a prompt enrichment of the Galaxy in these elements, possibly by early generations of massive stars. Particular attention to the Galactic evolution of elements produced by neutron-capture nucleosynthesis was given by Mathews, Bazan, & Cowan (1992), Pagel & Tautvaišienė (1997), and more recently by Travaglio et al. (1999). These authors adopted the standard approach to Galactic chemical evolution, assuming that stars form from a chemically homogeneous medium at a continuous rate. As stressed by Travaglio et al. (1999), this approach is able to reproduce spatially averaged values of element abundances over the Galactic age, but a more realistic model for the chemistry and dynamics of the gas is needed in order to investigate the earliest phases of halo evolution.

Recently, several studies have attempted to follow the enrichment history of the Galactic halo with special emphasis to the gas dynamical processes occurring in the early Galaxy: Tsujimoto, Shigeyama, & Yoshii (1999) provided an explanation for the spread of Eu observed in the oldest halo stars in the context of a model of supernova-induced star formation; Ikuta & Arimoto (1999) and by McWilliam & Searle (1999) studied the metal enrichment of the Galactic halo with the help of a stochastic model aimed at reproducing the observed Sr abundances; Raiteri et al. (1999) followed the Galactic evolution of Ba by means of a hydrodynamical N-body/SPH code; finally, Argast et al. (2000) concentrated on the effects of local inhomogeneities in the Galactic halo produced by individual supernova events, accounting

in this way for the observed scatter of some (but not all) elements typically produced by Type II supernovae.

In this paper we investigate whether incomplete mixing of the gas in the Galactic halo can lead to local chemical inhomogeneities in the ISM of the heavy elements, in particular Eu, Ba and Sr. Our chemo-dynamical evolution model for the Galactic halo is numerically based on a Monte Carlo technique. Starting from a discrete distribution of gas clouds, it follows star forming regions, stellar enrichment as well as mixing processes, during the early time of the Galaxy. We also investigate the consequences of infall of halo gas onto the disk. Since accurate r-process yields cannot be obtained from current stellar models, in order to study the composition of the halo gas in these elements we use analytical calculations presented by Travaglio et al. (1999), summarized in Sect. 2.1.

Following the seminal paper by Searle & Zinn (1978), we represent the Galactic halo as an ensemble of interacting gas clouds of different chemical composition. At variance with other recent studies (e.g. Tsujimoto et al. 1999) focused on the analysis of *local* inhomogeneities within individual clouds, in our picture each cloud is assumed to be chemically homogeneous, and able to host independent episodes of star formation. Clouds are allowed to coalesce with each other, and to fragment in smaller units, thus modifying the initial mass distribution. A similar scenario has been developed recently by Smith (1999) to study the problem of the formation of Galactic globular cluster. According to Smith (1999), if the proto-Galactic halo was constituted of clouds of size $\sim$ 1 kpc and mass in the range 8×10^5–3×10^7 $M_\odot$, evolving by coalescence, star formation and fragmentation episodes, some properties of the Galactic globular clusters system could be easily explained (e.g. their lower cut-off in metallicity with respect to field stars, their chemical homogeneity, etc.). In the present paper we do not investigate explicitly the formation of globular clusters, but we assume instead that stars formed in our clouds become part of the halo field star population.

The paper is organized as follows: in Sect. 2 we summarize the main characteristics of our chemo-dynamical model, the adopted stellar yields and the IMF; in Sect. 3 we discuss the effects of episodic infall of metal-deficient gas from the halo to the disk; in Sect. 4 we present a series of test calculations as preliminary applications of the Monte Carlo model presented here (i.e. a comparison with a "simple model" of chemical evolution, the G-dwarf distribution, and the evolution of the mass spectrum of coalesced interstellar clouds). In Sect. 5 we show the resulting age-metallicity relation, the abundances of Eu, Ba, and Sr at the early epochs of the evolution of the Galaxy, and we compare the model predictions with observations. Finally, in Sect. 6 we briefly summarize the conclusions of our work, indicating the constraints on the production of the r-process elements implied by our analysis, and suggesting possible direction for future investigations.

2. A Stochastic Model for the Galactic Halo

The main characteristics of the chemo-dynamical model presented in this paper (summarized in Table 1) are a realistic treatment of chemical inhomogeneities in the ISM due to incomplete mixing of stellar ejecta, and the occurrence of discrete episodes of star formation localized in time and space. We represent the halo gas by a ensemble of clouds of different chemical composition, assumed uniform inside each cloud. The idea that interstellar clouds collide and grow by coalescence (process in which clouds grow by accretion and interactions between other clouds and become progressively more massive and condensed) was first suggested by Hoyle (1953) and Oort (1954). The cloud population undergoes episodes of coalescence, fragmentation and star formation bursts. These processes are halted when the cloud reaches a critical mass $M_{\rm cr}$ at which it becomes gravitationally unstable and forms stars. In the present work, we consider the halo composed of discrete gas clouds and we follow their evolution during the early epoch of the Galaxy. To follow each coalescence episode, we select one cloud and choose randomly another cloud with a probability depending on the mass of the two clouds and on their collision cross section σ_{ij}. This selection of pairs of clouds at a certain timestep continues until all the clouds are examined, and occurs with a mixing frequency $f_{\rm m}$. The collision probability between two clouds of mass M_i and M_j is defined as

$$P_{ij} = \frac{\sigma_{ij}}{\sigma_{\rm max}} g(M_i, M_j), \tag{1}$$

where

$$g(M_i, M_j) = \frac{M_i M_j}{M_{\rm max}^2} \tag{2}$$

is a cut-off function adopted in order to minimize the probability of uninfluential collisions between a low-mass and a high-mass cloud. The probability P_{ij} is normalized to the values of the mass $M_{\rm max}$ and cross section $\sigma_{\rm max}$ of the most massive cloud at each timestep.

The clouds are assumed to be spherical with constant density, and the effective collision cross section σ_{ij} is proportional to the geometrical cross section

$$\sigma_{ij} \propto R_i^2 + R_j^2, \tag{3}$$

where R_i, R_j are the radii the clouds i and j. Observations suggest the existence of a mass-radius relation of present-day molecular clouds (e.g. Blitz 1993) in the Galactic disk

$$M \propto R^2, \tag{4}$$

resulting in a collision cross section linearly proportional to sum of the masses of the clouds

$$\sigma_{ij} \propto M_i + M_j, \tag{5}$$

TABLE 1
PARAMETERS OF THE STANDARD MODEL

initial number of clouds N	10^4
total initial mass $M_{\rm halo}$	$5 \times 10^{10}\ M_\odot$
initial mass range of clouds	10^3–$10^7\ M_\odot$
burst frequency $f_{\rm b}$	$5 \times 10^{-7}\ {\rm yr}^{-1}$
mixing frequency $f_{\rm m}$	$2.5 \times 10^{-7}\ {\rm yr}^{-1}$
star formation timescale t_0	2×10^7 yr
critical cloud mass $M_{\rm cr}$	$10^4\ M_\odot$
star formation efficiency η	0.03
IMF	Salpeter 0.1–120 $M_\odot$
mass range of SNII	8–120 $M_\odot$
e-folding time of disk accretion	10^9 yr

which is the expression for the collision cross section adopted in this paper. The new cloud formed in this coalescence episode has a mass equal to the sum of the masses of the two parent clouds, chemical composition equal to their mass-averaged chemical compositions, and zero age. Each new cloud formed at a certain timestep is not allowed to participate again in coalescence episodes at the same timestep. As a result of the process of coalescence, more massive clouds are produced at each timestep until they reach a critical value $M_{\rm cr} = 10^4\ M_\odot$ at which they are allowed to form dense molecular cores and give birth to clusters of stars. We assume a star formation efficiency $\eta = 0.03$ in each cloud, i.e. each burst converts 3% of the mass of the parent cloud M into stars.

Following a stellar burst, a cloud breaks up into a distribution of smaller clouds, due to the energetic processes that accompany star formation. Numerical calculations of the fragmentation process favour a small number of fragments ($\sim$ 2 to 5) per fragmentation stage (see e.g. Scalo 1985). We assume therefore that the original cloud produces a random number of fragments from 1 (no fragmentation) to 5 fragments (maximum fragmentation) characterized by the same chemical composition of the parent cloud. The age of the newly created cloud fragments is reset to zero. To estimate the timestep for the fragmentation episode we assume that, since the free-fall time in a molecular cloud is $\sim 10^6$ yr, stars are not allowed to form on a timescale smaller than $\sim 10^6$ yr. Observations and theory suggest that low- and intermediate-mass stars form within dense cores of molecular clouds on a timescale of $\sim 10^7$ yr (e.g. Shu et al. 1993). Hence we assume that the probability of a star formation burst (whenever the cloud's mass is higher than $10^4\ M_\odot$) is a Gaussian function

of the cloud's age t

$$P(t) = C \exp\left[-\left(\frac{t - t_0}{t_0}\right)^2\right], \tag{6}$$

with $t_0 = 2 \times 10^7$ yr. As shown in Table 1, the star formation rate (hereafter SFR) in our model occurs with a frequency $f_{\rm b} = 5 \times 10^{-7}$ yr^{-1}.

The SFR, under our assumptions, depends linearly on the mass of the most massive clouds. An order-of-magnitude value of the SFR can be estimated from the ratio between the mass of the gas able to form stars and the timescale of evolution of the Galactic halo. If one assumes that the baryonic mass of the Galactic halo is $\sim 5{\times}10^{10}$ $M_\odot$, and the efficiency of star formation is a few percent, the mass converted in stars in the Galactic halo is a few 10^9 $M_\odot$. For the lower limit of the timescale of evolution of the halo we can use the free-fall time $\tau_{\rm ff}$. Following the pioneering work by Eggen, Lynden-Bell & Sandage (1962), and the work by Fall & Rees (1985), assuming a pre-existing dark halo of radius R, which would account for the observed flat rotation curve of rotational velocity $v_{\rm c} \simeq 220$ km s^{-1}, then $\tau_{\rm ff}$ is given by

$$\tau_{\rm ff} = 2.8 \times 10^8 \left(\frac{R}{50 \text{ kpc}}\right) \text{ yr}. \tag{7}$$

For the star formation timescale in the halo we can use the range between $\tau_{\rm ff}$ and $\sim 4\tau_{\rm ff}$. Therefore, the expected SFR, given by the ratio (mass converted into stars)/$\tau_{\rm ff}$, is of order a few $M_\odot$ yr^{-1}.

We have explored different ranges for the initial mass of the clouds (the initial distribution of the clouds in this mass range being always chosen randomly), finding that a range of 10^3–10^5 $M_\odot$ leads to an average SFR which is too low (with an average value at 0.01 $M_\odot$ yr^{-1}), as shown in Fig. 1 (upper panel). An average SFR of ~ 1.5 $M_\odot$ yr^{-1} can be obtained starting with an initial mass range between 10^3–10^7 $M_\odot$ as shown in Fig. 1 (lower panel). We also found that SFR is linearly proportional to the efficiency η and to the ratio $f_{\rm m}/f_{\rm b}$. Then, to obtain a SFR of order a few $M_\odot$ yr^{-1} with the lower mass range of clouds (10^3–10^5 $M_\odot$) we need extreme values of η (~ 1) or $f_{\rm m}/f_{\rm b}$ ($\sim 10^3$ times higher than our standard values reported in Table 1).

As suggested earlier by Talbot & Arnett (1973) and Edmunds (1975), the timescale for the mixing of gas in the Galaxy, associated with random motions of the clouds, can be longer than the star formation time scale. In fact, the extent of dilution which occurs before stars form depends upon the interval between the supernova events and the next star formation event, and it depends upon whether mixing will occur throughout this time interval. For the simulations presented here we have explored different choices for the frequency of coalescence with respect to the burst frequency (as will be discussed below), concluding that $f_{\rm b} \sim 2f_{\rm m}$

represents the best value.

In this work we start with $N = 10^4$ clouds, randomly distrubuted in the mass range 10^3–10^7 $M_\odot$, and with a total mass $M_{\rm halo} = 5 \times 10^{10}$ $M_\odot$. The mass spectrum of the stars formed in the burst is described by a Salpeter stellar initial mass function (hereafter IMF)

$$\frac{d\mathcal{N}}{dm}(m) = Am^{-2.35}, \tag{8}$$

where m is the mass of the star in solar masses and A is a normalization constant. If the range of stellar masses extends from 0.1 $M_\odot$ to 120 $M_\odot$, then A is be determined from the condition

$$\int_{0.1}^{120} m\frac{d\mathcal{N}}{dm}(m)dm = \eta M, \tag{9}$$

giving

$$A \simeq 5.1 \left(\frac{\eta}{0.03}\right)\left(\frac{M}{10^3\ M_\odot}\right). \tag{10}$$

The sensitivity of the results from the adopted IMF will be discussed below.

2.1. Adopted Stellar Yields

We concentrate in this paper on the early enrichment of the halo gas ($t \leq 1$ Gyr) in Fe and heavy elements, in which the dominant role is played by Type II SNe (SNII). Therefore we include only the contribution of SNII without considering Type Ia supernovae. The Fe yields of SNII are taken from Woosley & Weaver (1995, hereafter WW95), for the mass range 12–40 $M_\odot$ (model "A", with $Z = 10^{-4}Z_\odot$ and $Z = 0$), and the delayed contribution to the chemical enrichment of the halo gas from SNe of different masses is also taken into account.

As no calculation for progenitors more massive than 40 $M_\odot$ is available in WW95, for $m > 40$ $M_\odot$ we have explored various stellar nucleosynthesis calculations recently published for massive stars (e.g. Thielemann, Nomoto & Hashimoto 1996; Chieffi, Limongi & Straniero 1998; Portinari, Chiosi, & Bressan 1998; Woosley, Langer & Weaver 1995; Maeder 1992). The results shown in this paper are taken from Woosley, Langer & Weaver (1995) for a star of 60 $M_\odot$ and solar metallicity (model 7K) in order to have a self-consistent data set for a wide range of stellar masses.

The production sites of r-process elements still need to be unambiguously identified, despite the large number of recent studies (see e.g. the hydrodynamic simulations by Wheeler, Cowan & Hillebrandt 1998, and Freiburghaus et al. 1999), and quantitative estimates of the r-process yields are still not available. Tsujimoto et al. (1999), Ikuta & Arimoto (1999), and

TABLE 2
YIELDS AND ABUNDANCES OF EU, BA, AND SR ADOPTED IN THIS WORK

	Mass range ($M_\odot$)	⟨Yield⟩ ($M_\odot$)	Solar mass fraction (Anders & Grevesse 1989)
Eu	8–10	6.4×10^{-7}	3.74×10^{-10}
Ba	8–10	5.7×10^{-6}	1.56×10^{-8}
Sr	15–25	3.5×10^{-6}	5.16×10^{-8}

McWilliam & Searle (1999) deduced empirically the the r-process yields from the available observational data of the most metal-poor stars, whereas Travaglio et al. (1999) presented analytical estimates of the r-process yields independent of observations, treating the r-process as a *primary* process originating in SNII. In this approach, the so called r-residuals are derived after subtracting from the solar abundances the predicted s-fractions at $t = t_\odot$ (see Travaglio et. al. 1999 for details). At lower metallicities the r-process yield is assumed to be proportional to the oxygen yield of SNII.

In the present work, to follow the evolution of Ba and Eu, we adopt the r-process calculations for different metallicities presented by Travaglio et al. (1999). Moreover, as will be discussed in more detail, the spectroscopic observations of [r/Fe] as a function of [Fe/H] show a decline of [r/Fe] at lower metallicities, that can be naturally explained by a time delay between the O-rich (partly Fe-rich) material ejected by the more massive SNe ($m \geq 15\ M_\odot$), and the r-process material ejected by the lower mass SNe (8–10 $M_\odot$ with zero Fe production). This delay may reflect the differences in stellar lifetime, but can be amplified by non-instantaneous mixing processes in the ISM. Finally, we have introduced new assumptions to quantify the production of Sr from massive stars, discussed in more detail in Sect. 5.3. In Table 2 are summarized the averaged stellar yields calculated for this work for Eu and Ba (in the mass range 8–10 $M_\odot$), and for Sr (in the mass range 15–25 $M_\odot$).

2.2. The Stellar Initial Mass Function

Several observational studies have been carried out in order to establish space or time variations of the IMF in our Galaxy and their dependence on parameters such as the gas metallicity. The regions that have been studied with direct star counts so far include the local field star population in our Galaxy and many star clusters of all ages and metallicities in both our Galaxy and Magellanic Clouds. The IMF derived for field stars in the solar

neighbourhood exhibits a power-law decline with mass above $\sim 1\ M_\odot$ roughly consistent with the original Salpeter (1955) law (Miller & Scalo 1979, hereafter MS; for a more recent review, see e.g. Larson 1998). However, below this value, the IMF of field stars flattens, showing a possible broad peak at a few tenths of a solar mass in the number of stars per unit logarithmic mass interval. However, the IMF at these masses is uncertain because it depends, among other things, on the poorly constrained evolutionary history of the Galaxy.

In this paper we adopt a Salpeter IMF but we explore the sensitivity of the model results (in particular the age-metallicity relation and the G-dwarf distribution) to different choices of the IMF. For instance, adopting the analytical expression of the IMF given by MS, the role of low-mass and high-mass stars is respectively overestimated and underestimated compared with the Salpeter IMF. The ratio between the number of massive stars in the mass range 8–120 $M_\odot$ calculated with the MS IMF and the Salpeter IMF, for the same initial cloud mass, is

$$\frac{(\mathcal{N}_{8-120})_{\rm MS}}{(\mathcal{N}_{8-120})_{\rm Salpeter}} \simeq 0.03. \tag{11}$$

Since the only Fe stellar sources for the first Gyr of the evolution of the Galaxy are SNII in this mass range, with a MS IMF the metallicity versus time covers a lower range of values. In particular, with this model we obtained [Fe/H] values that converged at 1 Gyr at [Fe/H] $\simeq -3$, instead of [Fe/H] $\simeq -1.5$ as in the case of a Salpeter IMF. In addition, with a MS IMF (underlying all the other assumptions of the Monte Carlo model presented here), in order to reach a metallicity [Fe/H] $\simeq -1.5$, the efficiency of star formation has to be increased by a large factor, from 3% with the Salpeter IMF up to 60% with the MS IMF.

3. Infall

As first stressed by Larson (1972) and by Hartwick (1976), gas infall from the Galactic halo to the disk guarantees additional material available above the amount that has been consumed, sustaining the disk star formation for longer times. Theoretical constraints on the collapse of the Galactic halo can be obtained by comparing its evolutionary and dynamical timescales. Hydrodynamical simulations by Burkert, Truran & Hensler (1992), and by Truran & Burkert (1993) showed that if the proto-Galactic gas was initially shock heated to the virial temperature $T_{\rm vir} \sim 2 \times 10^6$ K (or if early energetic star formation had acted to heat the halo to its virial temperature), the cooling timescale would be $\sim 3 \times 10^9$ yr (see also Boehringer & Hensler 1989), which is larger than the free-fall timescale. This result indicates that energetic heating and cooling processes might play an important role in regulating the early stages of formation and collapse of the Galactic halo. These theoretical arguments suggest a halo formation and collapse timescale of the order of $\sim 10^9$ yr. The

available abundance data for field and globular cluster stars in our Galaxy, when interpreted in the context of the current knowledge of nucleosynthesis theory, allow interesting timescale constraints to be imposed on the earliest stages of Galactic evolution. The implied timescale of star formation and supernova nucleosynthesis activity in the halo of our Galaxy appears to exceed the best estimates of several 10^8 yr, available from dynamical arguments. It seems increasingly clear that a rather complex sequence of events as a result of hierarchical mergers defined the formation and early evolution of the Galactic halo and disk components. Future abundance studies, particularly for globular cluster and field stars, may reasonably be expected to provide critical clues to the nature of this evolution. In the model presented here we assume that the gas mass in the halo decreases exponentially with an e-folding time $\tau = 10^9$ yr. Following these assumptions, at 1 Gyr, when the residual gas mass is reduced by $\sim 40\%$, the metallicity is [Fe/H] $\simeq -2$.

4. Test Calculations

In this Section we present a series of test calculations as preliminary applications of the Monte Carlo model. In particular, the current gas fraction, the distribution of long-lived stars in metallicity (G-dwarf problem), as well as the evolution of the mass spectrum of interstellar clouds due to coalescence episodes, are used to determine the values of the free parameters of the model.

4.1. Test 1: Comparison with the "Simple Model" of Chemical Evolution

As a first test of our model, we compare the distribution of Fe abundance versus the gas fraction resulting from our Monte Carlo simulations and from a "closed box" model of Galactic evolution. The "closed box" model, as introduced by Tinsley (1974), is characterized by a SFR $\psi(t)$, total mass M_t and gas mass $M_g(t)$ in the form of gas, in the instantaneous recycling approximation (IRA). The system is closed, with $M_g(0) = M_t$. The evolution of gas mass and metal content is regulated by the following expressions

$$\frac{dM_g}{dt} = -(1 - R)\psi, \tag{12}$$

and

$$\frac{d}{dt}(M_g Z) = -Z(1 - R)\psi + P_Z\psi, \tag{13}$$

where R is the returned fraction of gas defined as

$$R = \int_{m_1}^{m_{\max}} [1 - d(m)]\phi(m)dm, \tag{14}$$

and P_Z is the primary metal production factor defined as

$$P_Z = \int_{m_1}^{m_{\max}} [q_c(m) - d(m)]\psi(m)dm. \quad (15)$$

In these expressions, $\phi(m)$ is the IMF, $d(m)$ defines the mass fraction which remains as a stellar remnant upon the death of the star (i.e. all the matter external to $d(m)$ is ejected in the ISM), and $q_c(m)$ corresponds to the fraction (in mass) of ^{4}He converted into C, O, and heavier species. The lower limit of these integrals m_1 is the turn-off mass, taken as $m_1 = 0.8\ M_\odot$ for a Galactic age of 15 Gyr. In our simulations we are interested only in the first Gyr of the evolution of the Galaxy, therefore we take $m_1 = 2\ M_\odot$. The upper limit is $m_{\max} = 120\ M_\odot$. A straightforward integration of eq. (12) and (13) gives, independently on the SFR,

$$Z = -\frac{P_Z}{1-R} \ln\left(\frac{M_g}{M_t}\right). \quad (16)$$

Inserting in eq. (12)–(15) the values of the stellar parameters adopted in our Monte Carlo model we obtain $R = 0.71$, $P_Z = 7.9 \times 10^{-4}$. In Fig. 2 we compare the predictions of eq. (16), shown by the continuous line with the results of the Monte Carlo model (open circles). For the latter, the average Fe abundance was computed by summing the Fe mass in all clouds and dividing by the total mass of gas at various timesteps (infall was turned off in this simulation). The analytical results approximate very well the abundance of Fe computed numerically with the Monte Carlo model. In fact the IRA approximation, implicitly adopted in the equations of the "simple model", is satisfied to a very high degree in our Monte Carlo simulation, since the time evolution of the system ($\sim 10^9$ yr) is much larger than the lifetime of the lower mass SNII stars ($\sim 10^7$ yr). However, the analytical calculations can only predict the average Fe composition at each timestep, while our Monte Carlo model can follow the evolution of metallicity distribution of the halo clouds.

4.2. Test 2: the G-dwarf Distribution

The stars of spectral type G and luminosity corresponding to the dwarf class are low-mass stars ($m \simeq 0.8\ M_\odot$) evolving on a timescale of about 15 Gyr, comparable to the estimated age of the Galaxy. Therefore, they represent a sample that has never been affected by stellar evolution, accumulating since the first episodes of low-mass star formation. The paucity of metal-poor stars in the solar neighbourhood relative to the predictions of simple models of chemical evolution was noted by van den Berg (1962) and discussed further by Schmidt (1963) (see also Larson 1998). The G-dwarf problem has recently been found also in other galaxies, including ellipticals (Bressan, Chiosi & Fagotto 1994; Vazdekis et al. 1996; Worthey, Dorman & Jones 1996). To obtain the G-dwarf distribution we proceed in the

following way. Given the star formation rate $\psi(t)$ at a certain time t and defining as φ_G the fraction of G-dwarfs in a single stellar generation, the number $\mathcal{N}(z_1, z_2)$ of G-dwarfs with $z_1 \leq$ [Fe/H] $\leq z_2$ is obtained as

$$\mathcal{N}(z_1, z_2) = \varphi_{\rm G} \int_{t(z_1)}^{t(z_2)} \psi(t) dt, \tag{17}$$

where $t(z)$ is the time at which [Fe/H]$= z$.

The halo metallicity distribution function provides direct information about the initial stages of galaxy formation as it is sensitive to the bulk chemical properties of the interstellar gas from which the earliest generation of stars were born. A compilation of the relative numbers of low metallicity stars in the halo enables comparisons with alternative models of Galactic chemical evolution, and can be used to place constraints on the primordial rate of SNII, the SFR, and the time scale for the element enrichment in the early Galaxy. Early attempts to address this problem were based on the metallicity distribution of globular clusters determined by Hartwick (1976) (see also Bond 1981). Recent extensive observational campaigns by by e.g. Laird, Carney & Latham (1988), Ryan & Norris (1991), Beers, Preston & Shectman (1992), Carney et al. (1994), and Beers et al. (1998) have largely extended and updated the original data set. In particular, Beers and coworkers have identified several hundreds of stars belonging to the halo (and possibly thick disk) population of the Galaxy, and combined these data with other samples of extremely metal-deficient stars (Ryan & Norris 1991; Beers et al. 1992; Carney et al. 1994) to form a large database of low metallicity stars. In this work, we take as a reference the sample of low metallicity, high galactic latitude halo stars obtained by Beers et al. (1998, see their Fig. 2).

A comparison between the predictions of the Monte Carlo model for four different values of the mixing frequency $f_{\rm m}$ and the observational results by Beers et al. (1998) is shown in Fig. 3. The errorbars for the observational data indicate the $\sqrt{N_{stars}}$ noise associated with each bin. We also show in the same Figure the G-dwarf distribution obtained with the simple model of chemical evolution in the IRA approximation. The best fit to the observations is for the case $f_{\rm m} \simeq 2 f_{\rm b}$ which is assumed hereafter as the *standard* for our simulations. For larger values of this ratio, the metallicity distribution predicted by our model shows a substantial excess of stars below [Fe/H] $\simeq -3$ as compared with observations. In fact, lower metallicity clouds form through coalescence episodes with clouds of primordial abundance (higher metallicity clouds result from internal bursts of star formation), and increasing $f_{\rm b}$ with respect to $f_{\rm m}$ results in the creation of more low-metallicity clouds (and consequently low metallicity stars). At [Fe/H] $\simeq -2.5$ a contribution from thick disk stars can affect to the model predictions.

4.3. Test 3: Coalescence and the Evolution of the Cloud Mass Spectrum

In this Section we consider the evolution of the mass spectrum for interstellar clouds as a result of coalescence episode alone, without considering star formation and cloud fragmentation, in order to test our model against well-known analytical results for the evolution of the cloud mass spectrum under these circumstances (see e.g. Silk & Takahashi 1979). For instance, Hayashi & Nakagawa (1965) found that with a collision cross section scaling as $\sigma(M_1, M_2) \propto M_1^{\lambda/2} M_2^{\lambda/2}$ the solution of the coagulation equation must approach asymptotically the similarity solution defined by

$$t^{\frac{4+\lambda}{2-\lambda}} N(M,t) = f(t^{-\frac{2}{2-\lambda}} M). \tag{18}$$

Since $\lambda = 1$ in our standard case (see Sect. 2 for discussion), we expect the mass spectrum to evolve toward a limiting form

$$t^5 N(M,t) = f(t^{-2} M). \tag{19}$$

We start our simulations with $N = 10^4$ clouds with the same mass $M = 10^3\ M_\odot$, and we follow the evolution of the mass spectrum for a certain number of timesteps N_{ts}, until the cloud mass spectrum reaches a quasi equilibrium distribution. As mentioned above, the coalescence episodes are regulated by selecting one cloud and choosing randomly another cloud, with a probability that depends on the mass of the two clouds and on their collision cross section. This selection of pairs of clouds at a certain timestep continues until all clouds are examined and have had the possibility to be involved in a coalescence episode at a certain timestep. We show in Fig. 4 the resulting values of $t^5 N(M,t)$ vs. $t^{-2} M$ at different timesteps. The shape of the mass spectrum is clearly converging, after the first few timesteps, toward a shape-invariant form that depends only on the assumed dependence of the collision cross section on the masses of the clouds.

5. Results for the Chemical Evolution of the Galactic Halo

In this Section we present the results for the age-metallicity relation and for the abundances of Eu, Ba and Sr in the first Gyr of the Galaxy, by considering their r-process contributions only. Being essentially a pure r-process element, Eu is clearly a diagnostic for the chemical enrichment of the gas by r-process products. For Ba and Sr one has to disentangle the s- and r-process contribution weighted on the relative stellar sources at different times during the evolution of the Galaxy. On the other hand, Ba and Sr are observable at [Fe/H] $\simeq -4$, whereas Eu is observable only to [Fe/H]$\simeq -3$, hence predictions and models for the evolution in the halo gas of Ba and Sr are better testable than Eu.

In the following, we show the results obtained with our Monte Carlo model for Fe, for the Fe-group elements Mn and Co, and for the heavier elements Eu, Ba and Sr vs. [Fe/H] in the halo gas, discussing also the effect of variations of the standard values of the free parameters of our model.

5.1. Age-Metallicity Relation

From an observational perspective, the age-metallicity relation (hereafter AMR) for stars in the solar neighbourhood (mostly disk stars) was first determined by Twarog (1980), and later reanalyzed by Meusinger et al. (1991). A more recent study for the disk AMR, based on a new sample of nearby F and G dwarfs, was performed by Edvardsson et al. (1993) using high resolution spectra to determine the surface chemical composition of these stars. Their results show clearly that the concept of a well defined tight age-metallicity relation is unfounded: the slope of [Fe/H] vs. age over the lifetime of the Galactic disk is flat with a large scatter in metallicity at all ages. Unfortunately, a direct test of the age-metallicity relation for halo stars is not possible, since accurate age determinations are not available for this stellar population.

In Fig. 5 we show the results for the distribution of [Fe/H] versus time in the Galactic halo for different choices of the ratio $f_{\rm m}/f_{\rm b}$, obtained with the values of the parameters listed in Table 1 and described in Sect. 2. It is clear that a well defined AMR has to be replaced by a statistical relation. From Fig. 5 one can notice that after about 10^7 yr the spread in [Fe/H] increases, covering a range $-6 <$ [Fe/H] < -2. This is due to coalescence episodes between clouds that experienced at least one burst of star formation and clouds that never experienced star formation episodes. After a certain time which is of the order of $\sim 10^8$ yr, the halo gas starts to homogenize its chemical composition, and the spread in [Fe/H] is considerably reduced, converging to [Fe/H] $\simeq -2$. The time required for this "homogenization" depends clearly on the ratio $f_{\rm m}/f_{\rm b}$, ranging from $\simeq 10^8$ yr for the case $f_{\rm m} = f_{\rm b}$ to a few times 10^8 yr for the cases with higher $f_{\rm m}$. This fact might have relevant consequences on the distribution of [Eu/Fe], [Ba/Fe], and [Sr/Fe] vs. [Fe/H] as will be discussed in the following Section.

The distribution of [Fe/H] in the clouds is also influenced by the number of SNe that explode during each burst and by the mass distribution of clouds at each timestep. The upper limit on the cloud mass range has considerable consequences for the number of high-mass stars (50 to 100 $M_\odot$) formed during a star burst, since more massive clouds have more chance to form stars in the high-mass tail of the IMF (for a given efficiency η). This, in turns, affects the evolution of elements produced by massive SNe (e.g. oxygen), but has no consequences on the elements considered in this paper. In a forthcoming paper we will

consider quantitatively the processes limiting the growth of clouds by coalescence (tidal disruption, etc.) and the related aspects of massive stars nucleosynthesis.

With the adopted Salpeter IMF one can easily derive the number $\mathcal{N}_{\rm SN}$ of SNe that contribute to the minimal enrichment of [Fe/H] in a cloud

$$\mathcal{N}_{\rm SN} = \int_8^{120} \frac{d\mathcal{N}}{dm}(m)dm \simeq 0.13 \left(\frac{\eta}{0.03}\right) \left(\frac{M}{10^3\ M_\odot}\right). \qquad (20)$$

If $M = 10^4\ M_\odot$ (corresponding to the lowest mass allowed to form stars) and $\eta = 0.03$, one obtains $\mathcal{N}_{\rm SN} \simeq 2$. Ryan, Norris & Bessel (1991) argued that the ejecta of a single SN of 25 $M_\odot$ exploding in a 10^6 $M_\odot$ cloud is sufficient to enrich a cloud to [Fe/H] = −3.8. We find that the first enrichment episode by the most massive SNe result in [Fe/H] $\simeq -5$ after a few timesteps (at the first timesteps also the most massive SNe did not have enough time to contribute to the enrichment of the gas). At $t \sim 10^7$ yr the average metallicity has reached the value of [Fe/H] $\simeq -3$, due to the important contribution to Fe enrichment from $\sim 20\ M_\odot$ SNe. Ryan et al. (1991) maintained that the value of [Fe/H] = −3.8 sets a lower limit on the metallicity of the second generation of stars. Under the assumptions adopted for this work, as one can see in Fig. 5, Pop. II stars can reach lower values of [Fe/H] even at later times (up to [Fe/H] $\simeq -6$), due to efficiency of coalescence episodes between clouds with different chemical composition.

The highest values of metallicity reached with these simulations (shown in Fig. 5) at 10^9 yr are [Fe/H] $\simeq -1.8$. It is possible to reach higher [Fe/H] values by increasing the star formation efficiency above the standard value $\eta = 0.03$. In Fig. 5 is also shown for comparison (with a solid line) the age-metallicity relation obtained with the chemical evolution model presented by Travaglio et al. (1999). In Fig. 6 we show the age-metallitic distribution for the case $f_{\rm m} = 2f_{\rm b}$ with $\eta = 0.3$. For this case [Fe/H] reaches final values ~ 1 dex higher with respect to the case shown in Fig. 5 (*upper right panel*). Notice however that with a higher star formation efficiency the spread covered by the [Fe/H] distribution is higher, with significant consequences for the [Eu/Fe] and [Ba/Fe] distribution vs. [Fe/H], as will be discussed in the following Section.

As a final test of our model, we have considered the evolution of an ensemble of non-interacting interstellar clouds, switching off both coalescence and fragmentation. In this case, each cloud evolves as a closed box, continuosly enriched by episodes of star formation. The resulting age-metallicity relation shows no spread, demonstrating that the scatter shown in Fig. 5 is a result of mixing among clouds of different composition.

5.2. Iron-group elements: Co and Mn

As another test of the chemical evolution model described in this paper, we consider the gas enrichment (limited to the halo phase) of two of the most significant Fe-groups elements, Co and Mn. Although both the observed abundances and the theoretical yields of Fe-group elements are affected by large uncertainties, their study is of the highest importance to test chemical evolution predictions and to provide constraints on nucleosynthesis theory.

A remarkable result of recent observations of extremely metal-poor stars was the discovery of two different metallicity dependences of Fe-group element abundances (McWilliam et al. 1995b; Ryan, Norris, & Beers 1996): in particular, the two elements immediately below Fe, i.e. Cr and Mn, drop to high overdeficiencies at [Fe/H]< -2.5 (in terms of [X_i/Fe]), whereas elements above Fe, i.e. Co and possibly Ni, are seen to rise at higher values. However, one should keep in mind that the observational data can be affected by various uncertainties: for example, lines around ~ 4000 Åcan be blended with nearby strong Fe I lines, leading to different estimates of the Mn or Co abundance in the same objects. Also, the solar photospheric and meteoritic abundances of Mn differ by ~ 0.14 dex.

Both Mn and Co are synthesized mainly during explosive Si burning in SNe (products of ^{55}Co and ^{59}Cu decay, respectively). Therefore their yields are strongly affected by various factors like, e.g., the position of the mass cut between the neutron star and the ejecta, the total explosion energy and entropy, the delay time between the collapse and the explosion, etc.. Since we concentrate on the early stages of Galaxy evolution, we also need to take into account the dependence of Co and Mn yields on metallicity.

As discussed in Section 2.1, we concentrate on the early enrichment of the halo gas up to 1 Gyr of evolution, where the dominant role is played by SNII. We adopt the SNII yields from WW95 for the mass range 12–40 $M_\odot$ at $Z = 10^{-4} Z_\odot$ and at $Z = 0$ (three different explosive treatment are presented in WW95: as in Sect. 2.1, we use the models labelled "A", representing the standard explosive treatment). According to WW95, zero-metallicity models of 35 and 40 $M_\odot$ provide [Co/Mn] ratios similar to the higher metallicity models of corresponding mass, whereas the 25 and 30 $M_\odot$ moldels of zero-metallicity produce higher ratios (~ 1 dex). For these reasons, and given the difficulties in modelling the explosion of the most massive stars, we assume that only stars with $m \simeq 40\ M_\odot$ contribute to the enrichment of the proto-Galactic gas in Fe-group elements.

The results obtained with our stochastic model for the evolution of Co and Mn during the first Gyr of evolution of the Galaxy are shown in Fig. 7, compared with spectroscopic observations of metal-poor stars from McWilliam et al. (1995b) and Ryan et al. (1996) (stars observed by both authors are connected by dotted lines). For the extremely metal-poor

star CS 22876-032 (with [Fe/H] = −3.71), recent spectroscopic data by Norris, Beers, & Ryan (2000) indicate a metallicity higher than the values estimated by Ryan et al. (1996) because of the decomposition of the spectrum into two components (the star has been classified as double line spectroscopic binary), and a much lower Mn abundance.

5.3. Europium and Barium Enrichment in the Halo Gas

The scatter observed in the relative abundances of neutron capture elements with respect to iron, e.g. [Eu/Fe] and [Ba/Fe], is often interpreted as an evidence for the inhomogeneous enrichment of the ISM at the very beginning of the evolution of the Galaxy. The abundance distribution of [Eu/Fe] provides a direct way to address this problem, since Eu is mostly produced by r-process nucleosynthesis. For Ba, the contribution of s-process nucleosynthesis from AGB stars in the mass range 2–4 $M_{\odot}$(hereafter low-mass stars, or LMS) accounts, at the epoch of solar formation, for 80% of the known abundance (for more details see e.g. Travaglio et al. 1999, Gallino et al. 1998), whereas only $\sim 20\%$ comes from the r-process.

The quantitative estimates for the r-process yields of Eu and Ba are taken from Travaglio et al. (1999). These authors explored different SNe mass range for the production of r-process in the contest of a chemical evolution model. They noticed that in order to reproduce the typical increasing trend of [Ba/Fe] and [Eu/Fe] at [Fe/H] $\simeq -1.5$, the production of Fe at low metallicity must have occurred mainly before the production of r-process component of Ba and Eu. According to their model, SNII in the mass range 8 – 10 $M_{\odot}$ appear to be good candidates for the primary production of r-nuclei, whereas a range extending to much higher masses seems to be in conflict with the available observations. As noticed by the authors, the assumption of r-process from low-mass SNe is also supported by recent theoretical models by Wheeler et al. (1998) and Freiburghaus et al. (1999).

For this work we adopt the same assumptions on the r-process yields from SNII in the mass range 8–10 $M_{\odot}$, as listed in Table 2. In Fig. 8 we show the results of the Monte Carlo model for the Eu enrichment in the halo gas from 8–10 $M_{\odot}$ at different metallicities. This Figure provides more insight into the age at which the halo gas begins to be enriched by the r-process, as well as the metallicity range that star forming clouds enriched in Eu can cover at a given epoch. In fact one can see that the first enrichment of Eu in the clouds starts at [Fe/H] $\simeq -5$, corresponding to $\sim 10^8$ yr. This delay is due to the choice of the SNe mass range for the production of r-process. At [Fe/H] $\simeq -2$, the Eu composition is mostly homogenized (for the last 10^8 yrs). In this Figure is also shown for comparison (with a solid line) the chemical enrichment of Eu obtained with the Travaglio et al. (1999) model. One can see that the higher X(Eu) values obtained with the Monte Carlo model at 10^8–10^9 yr are

well matched by the average X(Eu) value obtained with the Travaglio et al. (1999) model. However with the Monte Carlo model the gas is enriched in Eu since lower metallicities. In fact with the Monte Carlo model we can simulate clouds enriched in Eu at [Fe/H] $\simeq -5$ but formed at later times with respect two clouds with higher [Fe/H].

The Eu enrichment in the halo gas is also shown in Fig. 9, together with the Ba enrichment, in terms of [Eu/Fe] and [Ba/Fe] vs. [Fe/H], compared with spectroscopic observations. The observational sensitivity limit for Eu and Ba is given by [Eu/H] $\simeq -4 \div -3$ and [Ba/H] $\sim -6 \div -5$ (Gratton, private communication), and is shown by a long-dashed lines. At [Fe/H] $\simeq -2$ the Eu and Ba enrichment of the gas has dropped (i.e. the contribution of the 8–10 $M_{\odot}$ has vanished), and the Fe composition started to be dominant. This results in a decrease of [Eu/Fe] and [Ba/Fe] at [Fe/H] ≥ -2, and a contribution from the thick disk is required. At [Fe/H] $\simeq -2$ an additional (and dominant) contribution to Ba from s-process nucleosynthesis in low-mass AGB stars is also required (as shown by Gallino et al. 1998 and Travaglio et al. 1999, the complex behavior of the s-element yields as a function of metallicity allows them to dominate the Galactic enrichment only at [Fe/H] ≥ -2).

As discussed in the previous Section and shown in Fig. 6, a higher SF efficiency (e.g. 30% of the mass of the clouds converted in stars) will increase the final [Fe/H] at 1 Gyr up to $\sim$ 1 dex. The effect on [Eu/Fe] and [Ba/Fe] is shown in Fig. 10, where one can see that the Monte Carlo model predicts a spread in [Eu/Fe] and [Ba/Fe] composition where the observations show a more homogeneous composition.

Following the discussion presented by Travaglio et al. (1999), we have also explored different SNII mass ranges for the production of r-process elements. We show in Fig. 11 the result obtained under the assumption that r-process nucleosynthesis occurs in 15–30 $M_{\odot}$ SNII. In this case the enrichment of the gas in Eu and Ba starts at earlier times with respect to the simulation shown in Fig. 8, due to the shorter lifetimes of this SN mass range. However, the fraction of stars in this mass range, as well as the r-process yields, produce an average value of [Eu/Fe] and [Ba/Fe] vs. [Fe/H] which is higher than the case with a low SNII mass range. This result is in disagreement with the observed values of [Eu/Fe] and [Ba/Fe]. The only exception is represented by the peculiar star CS 22892-052 (where r-process elements are enhanced over about 40 times the solar value), characterized by [Fe/H] $\simeq -3$, [Eu/Fe] $\simeq +1.44$, and [Ba/Fe] $\simeq +0.93$. With the r-process yields adopted here these values are in general not reproduced, unless the r-process come from higher mass range SNII (as shown in Fig. 11), at the price of not reproducing the abundances observed in the other stars.

We have also explored the consequences of zero Fe yields for higher mass stars. From the point of view of stellar evolution, this is supported by the idea that mass-loss increases with metallicity (the efficiency of radiation pressure driven wind scales with metallicity as

$\dot{M} \propto Z^{0.5}$, see Kudritzki et al. 1989) and that the probability to have even less Wolf-Rayet stars that produce Fe is higher at lower metallicities. However, this will not affect considerably the results for the inhomogeneous composition of the gas at $t \geq 10^8$ yr, when Eu production starts. This is due to the short lifetimes of these massive stars which lead to chemical enrichment of the ISM on a shorter timescale ($\simeq$ few times 10^6 yr).

5.4. Strontium Enrichment in the Halo Gas

The study of the chemical evolution of Sr deserves a deeper analysis and special comments. A large number of metal-poor stars with [Fe/H] ≤ -2.0 and $-1.5 \leq$ [Sr/Fe] $\leq +0.8$, shows a relative abundance of Sr that tends to decrease with an increase of iron abundance (see e.g. Ryan 2000, with references therein for a collection of data, and Burris et al. 2000). However, the estimate of the different sources that contribute to the Galactic evolution of Sr has not yet quantified in detail.

Gallino et al. (1999) analyzed the various contributions to the solar abundance of *s*-process elements, arguing that while low-mass AGB stars can account almost entirely for the heavy *s*-isotopes from Ba to Pb, they can contribute only $\sim 70\%$ of the solar composition of nuclei around Sr. The addition of *s*-process yields from intermediate mass AGB stars (with $m > 4\ M_\odot$, hereafter IMS) can play a relevant role in the Galactic nucleosynthesis of the elements across the Sr-Y-Zr peak and provide up to 15% of their solar system abundances (Gallino et al. 1999). We should however keep in mind that the mechanisms of production of *s*-process nuclei from IMS are not not completely elucidated and that detailed models have become available only very recently.

In the halo phase the effects of the AGB nucleosynthesis on the chemical enrichment of the ISM are less important with respect to the disk, due to the relatively long time scale required by their evolution. In the halo the production of heavy elements is mostly due to the *r*-process (see e.g. Truran 1981). High-mass stars also contribute to the Sr enrichment of ISM, via *r*-process nucleosynthesis (see e.g. Woosley et al. 1994), in addition to a small contribution by *s*-process from massive stars ($\sim$ 5%, according to Raiteri et al. 1993). The fact that the *r*-process is not as simple as currently assumed and requires different sites for producing nuclei respectively lighter and heavier that $A \simeq 140$ was first advanced by Wasserburg, Busso & Gallino (1996), but presnt-day stellar models are not yet able to quantify the production of these elements. Looking at the observations of Sr, the lower boundary of the observed [Sr/Fe] abundance can be explained by the "normal" *r*-process behaviour, corresponding to a universal [Ba/Sr] *r*-process value. An additional source is required to explain the large spread observed in [Sr/Fe], as for example a primary

component from massive stars. The observations of Sr strongly suggest that the process at work must involve low neutron exposures that synthesize only species around the atomic number of Sr, without reaching species with atomic number around Ba. The observations of other species near Sr, also enhanced in these high Sr stars (Ryan et al. 1996), provide additional evidence supporting this possibility.

To explore the spread in [Sr/Fe] vs. [Fe/H] that we can reproduce with the Monte Carlo model presented here, we summarize the contribution to Sr from different stellar sources during the evolution of the Galaxy, as discussed above:

(*i*) an *s*-component from LMS ($m \simeq 2$–$4\ M_{\odot}$), for $\sim 60\%$ of the the solar composition;

(*ii*) an *s*-component from IMS ($m \simeq 4$–$7\ M_{\odot}$), for $\sim 15\%$ of the solar composition;

(*iii*) an *s*-component from massive stars, called *weak-component*, for $\sim 5\%$ of the solar composition;

(*iv*) a primary component to be attributed to massive stars with $m \simeq 15$–$25\ M_{\odot}$, for $\sim 20\%$ at any time.

Notice that since (*iii*) is a secondary component, i.e. it needs an enrichment of the gas from a previous generations of stars, it is negligible at low metallicities.

Fig. 12 shows the result for [Sr/Fe] vs. [Fe/H] computed under these assumptions. Since we are interested in the early phases of evolution of the Galaxy we took into account only the Sr contribution from massive stars. The spread observed in low metallicity stars is well reproduced by the model up to [Fe/H] $\simeq -1.8$. As in Fig. 9 and Fig. 10 we plotted an observational limit for Sr given by [Sr/H] in the range $\simeq -6 \div -5$ (Gratton, private communication).

6. Conclusions

Spectroscopic abundance determinations in various samples of metal-poor halo stars reveal the presence of large dispersions in heavy elements. If the observed scatter is *intrinsic* (not substantially influenced by different calibration methods or data reduction procedures), this fact can be interpreted as a signature of incomplete mixing of the interstellar medium at the first epochs of the Galaxy.

In this work we have presented a chemo-dynamical model, based on a Monte Carlo technique, specifically devoted to study the inhomogeneous evolution of the Galactic halo. We have considered the effects of local enrichment of the halo gas by star formation episodes

in interstellar clouds, which subsequently *fragment* into smaller objects, as well as the *coalescence* between clouds. With this model we explored the SFR versus time, the interstellar mass function, the age-metallicity relation and the G-dwarf distribution. We have also discussed the effects of a term of exponential infall (with an e-folding time of 10^9 yr) from the halo gas to the disk, and the evolution of the mass spectrum of coalesced interstellar clouds.

The main parameters that control the dynamical evolution of the halo as well as the enrichment history of the halo ISM are the initial mass range of clouds (from 10^3 $M_\odot$ up to 10^7 $M_\odot$, chosen in order to obtain a SFR ~ 1 $M_\odot$/yr), the efficiency of star formation (a few percent of the mass of the clouds), and the frequency of coalescence episodes with respect to star formation (the standard choice for this work is $f_{\rm m} = 2f_{\rm b}$).

The main goal of the model is to follow the evolution of the halo metallicity and of the heavy elements Eu, Ba and Sr during the early ages of the Galaxy. Since this work is concentrated on the halo evolution, we have quantified the r-process contribution, using previous analytical calculations to derive the r-process yields introduced by Travaglio et al. (1999). The comparison of the model results with available spectroscopic data for Population II stars suggests a production of Eu and Ba from SNII, slightly delayed with respect to the main phase of oxygen enrichment, that can be explained in the context of low-mass (8–10 $M_\odot$) SNII.

Under these assumptions, the values of [Eu/Fe] and [Ba/Fe] cover a spread of ~ 3 dex up to [Fe/H] $\simeq -2$. At higher [Fe/H] (corresponding to $t \geq 4 \times 10^8$ yr), the gas has had enough time to homogenize its chemical composition and the large [element/Fe] spread is considerably reduced. Two interesting points should be noticed: first, the model predicts the existence of a large number of clouds with [Eu/Fe] and [Ba/Fe] values 1 or 2 dex lower than the observations, below the present-day threshold for spectroscopic observations of Eu and Ba (Gratton, private communication). Moreover, the model predicts halo gas with metal-enrichment of [Fe/H] < -4, but no stars are observed at such low metallicities. One possible explanation, is again the difficulty to observe objects with such a low metallicity; another possibility is a pre-enrichment of the halo gas by a Population III of massive stars.

We have also discussed the problem of chemical evolution of Sr. The production of this element was obtained under different assumptions with respect to Ba and Eu. Our explanation of the spread of [Sr/Fe] observed in low metallicity halo stars is that in addition to a s-contribution from LMS and IMS, and a s-contribution from massive stars (weak-component), there is a primary component from SNII with masses $\sim$ 15–25 $M_\odot$ accounting for $\sim 20\%$ of the Sr solar composition.

The research of C.T. and D.G has been supported in part by grant COFIN98-MURST

at the Osservatorio di Arcetri. C.T. would like to thank R. Gratton for kind comments about the spectroscopic observations, and A. Nelson for useful discussions at the beginning of this work.

REFERENCES

Anders, E., & Grevesse, N. 1989, Geochim. Cosmochim. Acta, 53, 197

Argast, D., Samland, M., Gerhard, O. E., & Thielemann, F.-K. 2000, A&A, 356, 873

Beers, T.C., Preston, G.W., & Shectman, S.A. 1992, AJ, 103, 1987

Beers, T.C., Rossi, S., Norris, J.E., Ryan, S.G., Molaro, P., & Rebolo, R. 1998, SSRv, 84, 139

Blitz, L. 1993, Protostars and Planets III, ed. E.H. Levy & J.I. Lunine (Tucson: Univ. Arizona Press), 125

Boehringer, H., & Hensler, G. 1989, A&A, 251, 147

Bond, H.E. 1981, ApJ, 248, 606

Bressan, A., Chiosi, C., & Fagotto, F. 1994, ApJS, 94, 63

Burkert, A., Truran, J.W., & Hensler, G. 1992, ApJ, 391, 651

Burris, D.L., Pilachowski, C.A., Armandroff, T.E., Sneden, C., Cowan, J.J., & Roe, H. 2000, ApJ, in press

Carney, B.W., Lathman, D.W., Laird, J.B., & Aguilar, R.A. 1994, AJ, 107, 2240

Chieffi, A., Limongi, M., & Straniero, O. 1998, ApJ, 502, 737

Cohen, J.G. 1982, ApJ, 258, 143

Da Costa, G.S. 1991, in The Magellanic Clouds and their Dynamical Interaction with the Milky Way, IAU Symp. 148, ed. Hayanes, R.F., Milne, D.G., (Dordrecht: Kluwer), p. 183

Edmunds, M.G. 1975, Ap&SS, 32, 483

Edvardsson, B., Andersen, J., Gustaffson, B., Lambert, D.L., Nissen, P.E., & Tomkin, J. 1993, A&A, 275, 101

Eggen, O.J., Lynden-Bell, D., & Sandage, A.R. 1962, ApJ, 136, 748

Fall, S.M., & Rees, M.J. 1985, ApJ, 298, 18

Ferrini, F., Matteucci, F., Pardi, C., & Penco, U. 1992, ApJ, 387, 138

Freiburghaus, C., Rembges, J.F., Rauscher, T., Kolbe, E., Thielemann, F.K., Kratz, K.L., Pfeiffer, B., & Cowan, J.J. 1999, ApJ, 516, 381

Galli, D., Palla, F., Ferrini, F., & Penco, U. 1995, ApJ, 443, 536

Gallino, R., Arlandini, C., Busso, M., Lugaro, M., Travaglio, C., Straniero, O., Chieffi, A., & Limongi, M. 1998, ApJ, 497, 388

Gallino, R., Arlandini, C., Busso, M., Lugaro, M., Travaglio, C., et al. 1999, in Nuclei in the Cosmos V, ed. N. Prantzos and S. Harissopulos, p.216, Paris: Edition Frontieres

Gilroy, K.K., Sneden, C., Pilachowski, C.A., & Cowan, J.J. 1988, ApJ, 327, 298

Gratton, R.G., & Sneden, C. 1994, A&A, 287, 927

Hartwick, F.D.A. 1976, ApJ, 209, 418

Hayashi, C., & Nakagawa, Y. 1975, Prog. Theoret. Phys., 54, 93

Hoyle, F. 1953, ApJ, 118, 513

Ikuta, C., & Arimoto, N. 1999, PASJ, 51, 459

Kudritzki, R.P., Pauldrach, A., Puls, J., & Abbott, D.C. 1989, A&A, 219, 205

Kunth, D., Lequeux, J., Sargent, W.L.W., & Viallefond, F. 1994, A&A, 282, 709

Laird, J.B., Carney, B.W., & Latham, D.W. 1988, AJ, 96, 1908

Larson, R.B. 1972, Nature, 236, 7

Larson, R.B. 1998, MNRAS, 301, 569

Maeder, A. 1992, A&A, 264, 105

Mathews, G.J., Bazan, G., & Cowan, J.J. 1992, ApJ, 391, 719

McWilliam, A., Preston, G.W., Sneden, C., & Shectman, S. 1995a, 431, L27

McWilliam, A., Preston, G.W., Sneden, C., & Searle, L. 1995b, AJ, 109, 2736

McWilliam, A. 1998, AJ, 115, 1640

McWilliam, A., & Searle, L. 1999, in Galaxy Evolution: Connecting the Distant Universe with the Local Fossil Record, ed. M. Spite, (Dordrecht: Kluwer), p. 133

Meusinger, H., Reimann, H.G., & Stecklum, B. 1991, A&A, 245, 57

Miller, G.E., & Scalo, J.M. 1979, ApJS, 41, 513

Norris, J.E., Beers, T.C., & Ryan, S.G. 2000, ApJ, 540, 456

Olsewski, E.W., Schommer, R.A., Suntzeff, N.B., & Harris, H.C. 1991, AJ, 101, 515

Oort, J.H. 1954, Bull. Astron. Inst. Netherlands, Vol.12. p.455

Pagel, B.E.J., & Tautvaišienė, G. 1997, MNRAS, 288, 108

Pilyugin, L.S. 1992, A&A, 260, 58

Portinari, L., Chiosi, C., & Bressan, A. 1998, A&A, 334, 505

Raiteri, C.M., Gallino, R., Busso, M., Neuberger, D., & Käppeler, F. 1993, ApJ, 419, 207

Raiteri, C.M., Villata, M., Gallino, R., Busso, M., & Cravanzola, A. 1999, ApJ, 518, L91

Ryan, S.G., & Norris, J.E. 1991, AJ, 101, 1835

Ryan, S.G., Norris, J.E., & Bessel, M.S. 1991, AJ, 102, 303

Ryan, S.G., Norris, J.E., & Beers, T.C. 1996, ApJ, 471, 254

Ryan, S.G. 2000, Proc. 35.th Liege Int. Astrophys. Coll. (Liege: Univ. de Liege Institute d'Astropysique), Eds. A. Noels, D. Fraipont-Caro, M. Gabriel, N. Grevesse, P. Demarque, p. 101

Salpeter, E.E. 1955, ApJ, 121, 161

Scalo, J.M. 1985, in Protostar & Planets II, ed. D.C. Black & M.S Matthews (Tucson: Univ. Arizona Press), 201

Schmidt, M. 1963, ApJ, 137, 758

Searle, L., & Zinn, R. 1978, ApJ, 225, 357

Shu, F.H., Najita, J., Galli, D., Ostriker, E., & Lizano, S. 1993, Protostars and Planets III, ed. E.H. Levy & J.I. Lunine (Tucson: Univ. Arizona Press), 3

Silk, J., & Takahashi, T. 1979, ApJ, 229, 242

Smith, G. H., 1999, ApJ, 526, L21

Sneden, C., Preston, G.W., McWilliam, A., & Searle, L. 1994, ApJL, 431, L27

Sneden, C., Cowan, J.J., Burris, D.L., & Truran, J.W. 1998, ApJ, 496, 235

Talbot, R.J., & Arnett, D.W. 1973, ApJ, 186, 69

Thielemann, F.-K., Nomoto, K., & Hashimoto, M. 1996, ApJ, 460, 408

Travaglio, C., Galli, D., Gallino, R., Busso, M., Ferrini, F., & Straniero, O. 1999, ApJ, 521, 691

Truran, J.W. 1981, A&A, 97, 391

Truran, J.W., & Burkert, A. 1993, Physics Reports, 227, 235

Tsujimoto, T., Shigeyama, T., & Yoshii, Y. 1999, ApJ, 431, L27

Twarog, B.A. 1980, ApJ, 242, 242

van den Berg, S. 1962, AJ, 67, 486

Vazdekis, A., Casuso, E., Peletier, R.F., & Beckman, J.E. 1996, ApJS, 106, 307

Wasserburg, G.J., Busso, M., & Gallino, R. 1996, ApJ, 466, L109

Wheeler, J.C., Cowan, J.J., & Hillebrandt, W. 1998, ApJ, 493, L101

Woosley, S.E., Wilson, J.R., Mathews, G.J., Hoffman, R.D., & Meyer, B.S. 1994, ApJ, 433, 229

Woosley, S.E., & Weaver, T.A. 1995, ApJ, 448, 315

Woosley, S.E., Langer, N., & Weaver, T.A. 1995, ApJ, 448, 315

Worthey, G., Dorman, B., & Jones, L.A. 1996, AJ, 112, 948

This preprint was prepared with the AAS LaTeX macros v4.0.

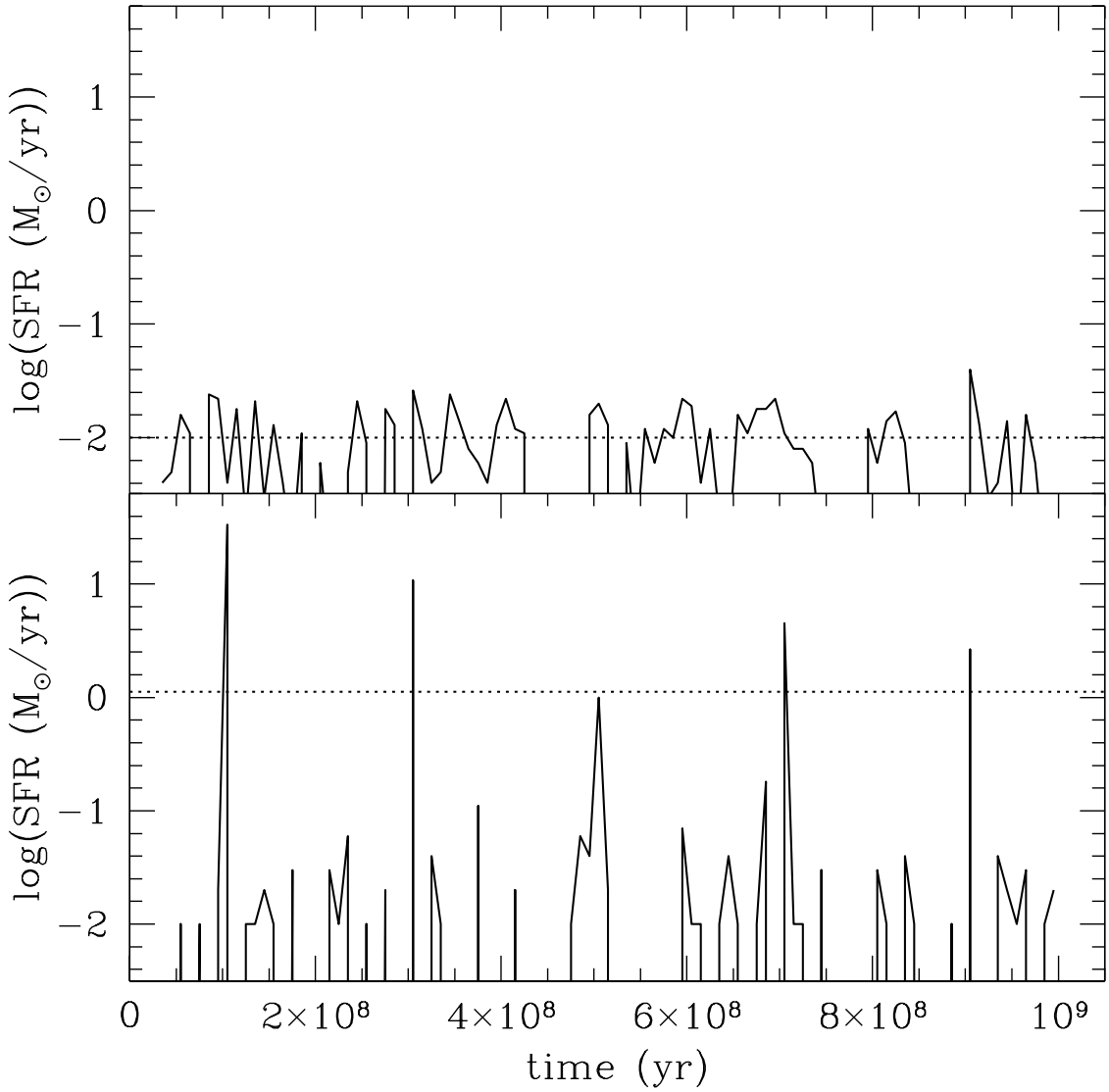

Fig. 1.— Star formation rate (in $M_\odot$ yr^{-1}) vs. time for two different assumptions on the initial mass of the clouds in the range 10^3–10^5 $M_\odot$(*upper panel*), and 10^3–10^7 $M_\odot$(*lower panel*). The *short-dashed* line represents the average value.

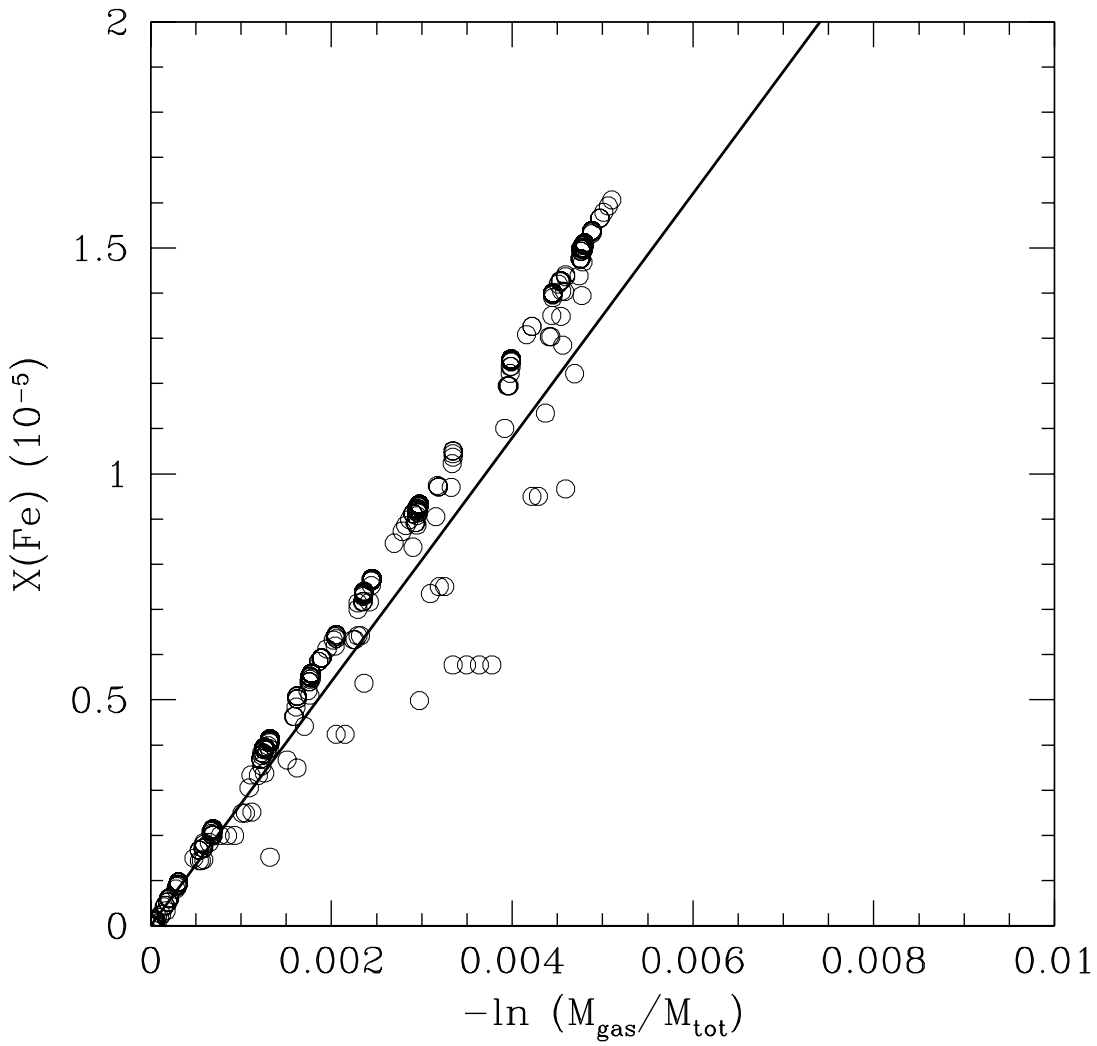

Fig. 2.— Abundance of Fe as function of the gas fraction for the Monte Carlo model without infall (*open circles*) compared with the simple closed box model in the IRA (*continuous line*). For the Monte Carlo model X(Fe) is computed as the sum of the Fe mass present in all the clouds divided by the total mass of the gas at each timestep.

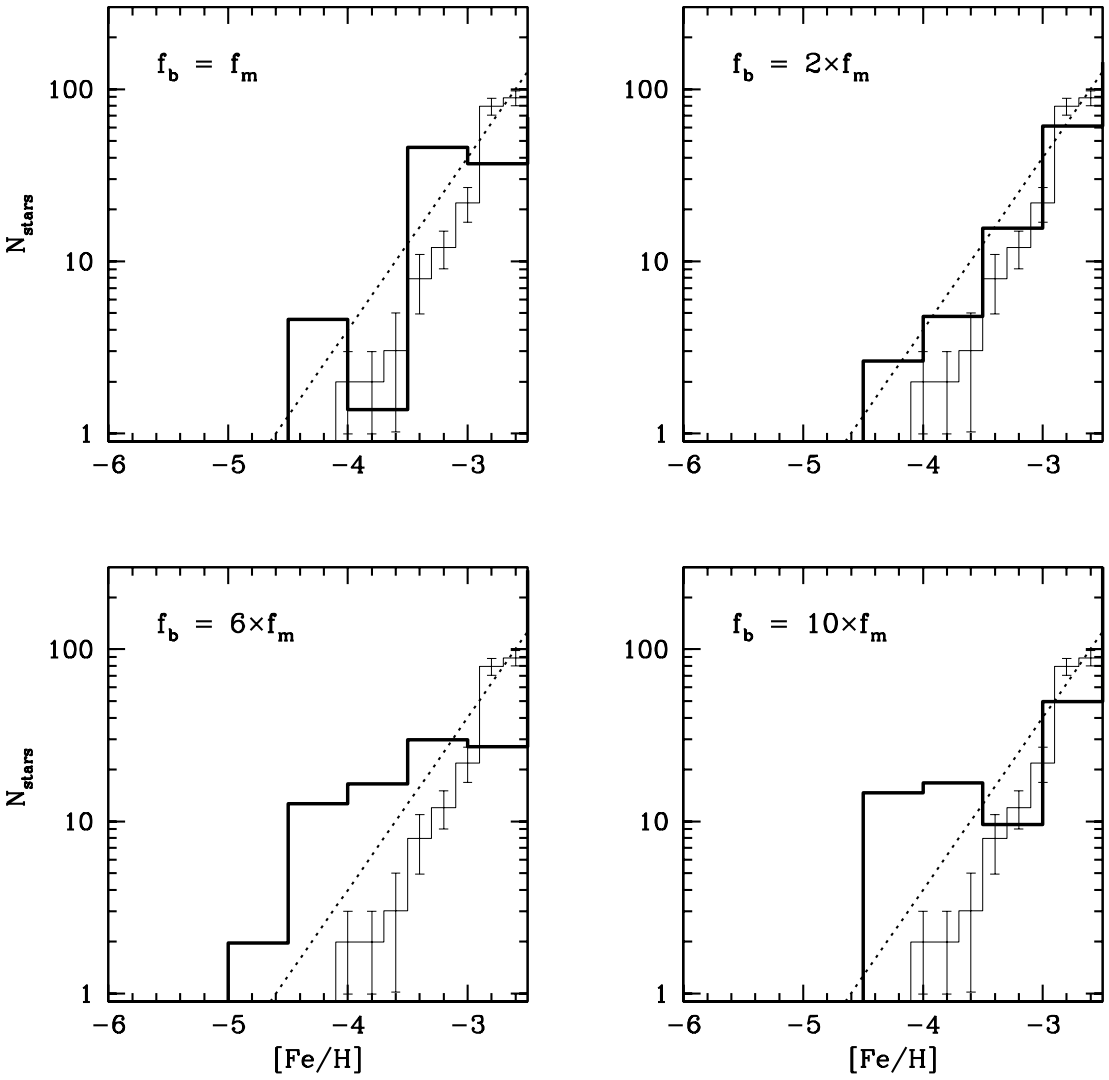

Fig. 3.— G-dwarf distribution for halo stars. The result of the Monte Carlo model (*solid line*) is compared with the collected sample of observations by Beers et al. (1998) (*dotted line*), and to the simple model of chemical evolution in the IRA approximation (*dashed line*). The errorbars for the observational data indicate the $\sqrt{N_{stars}}$ noise associated with each bin. The number of G-dwarf stars is plotted in arbitrary units. The four panels show four different choices for the ratio between the frequency of coalescence $f_{\rm m}$ and of star formation $f_{\rm b}$, as discussed in the text.

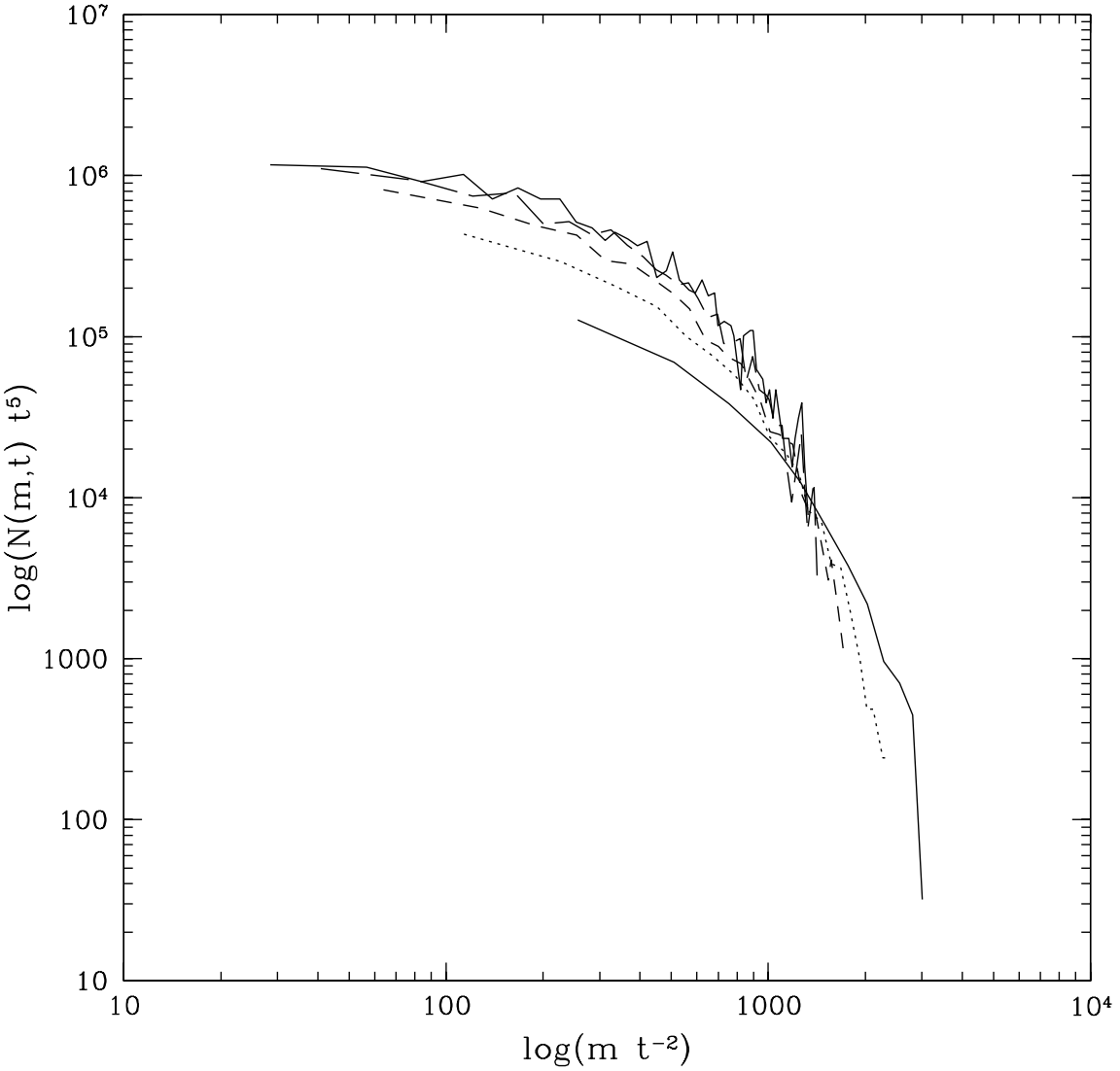

Fig. 4.— Evolution vs. time of the mass spectrum of coalesced interstellar clouds in a similarity solution according to eq. (19) in the text and for $\lambda = 1$. Different lines correspond to different timestep of evolution.

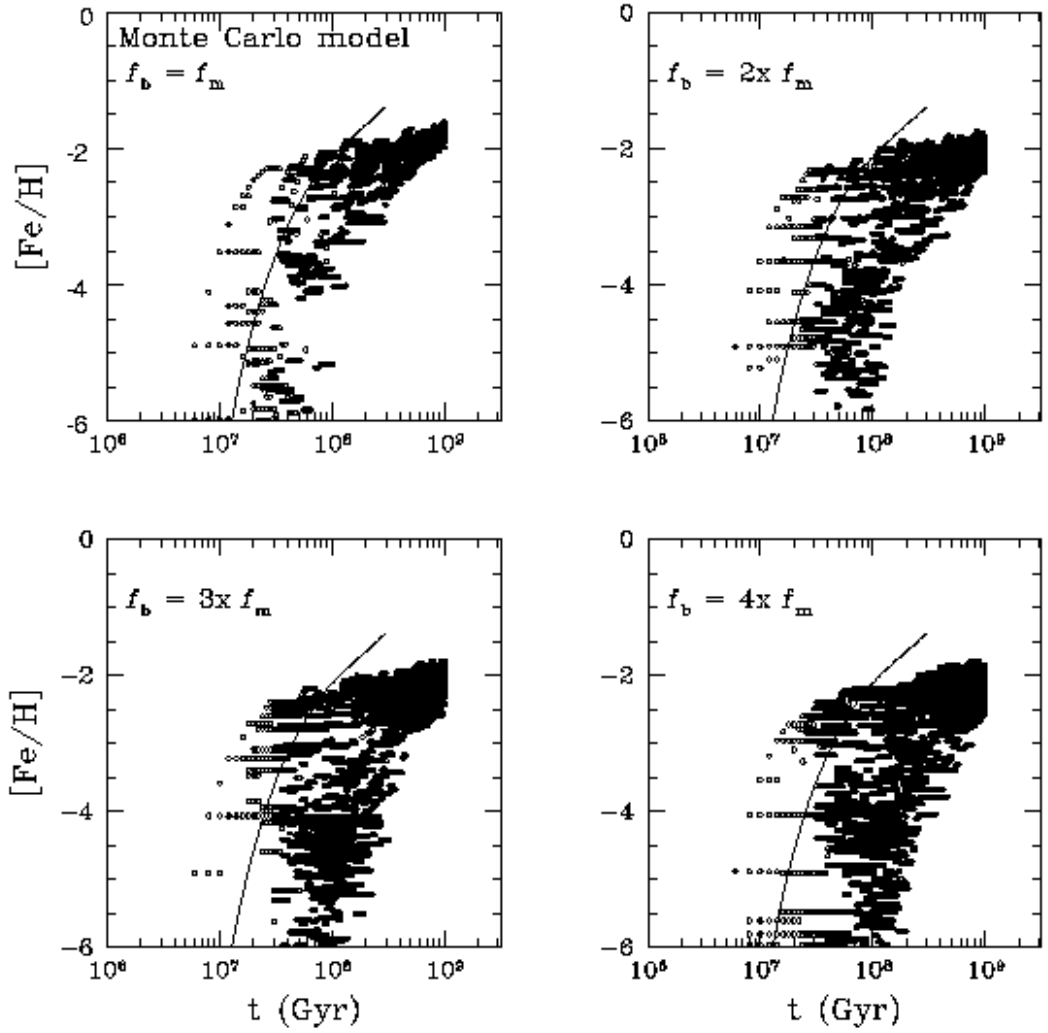

Fig. 5.— Distribution of metallicity vs. time obtained with the Monte Carlo model. The four panels show four different choices for the ratio between the frequency of coalescence $f_{\rm m}$ and of star formation $f_{\rm b}$, as discussed in the text. Points represent interstellar clouds during the first Gyr of the evolution of the Galaxy. Solid line represents the metallicity evolution obtained by Travaglio et al. (1999).

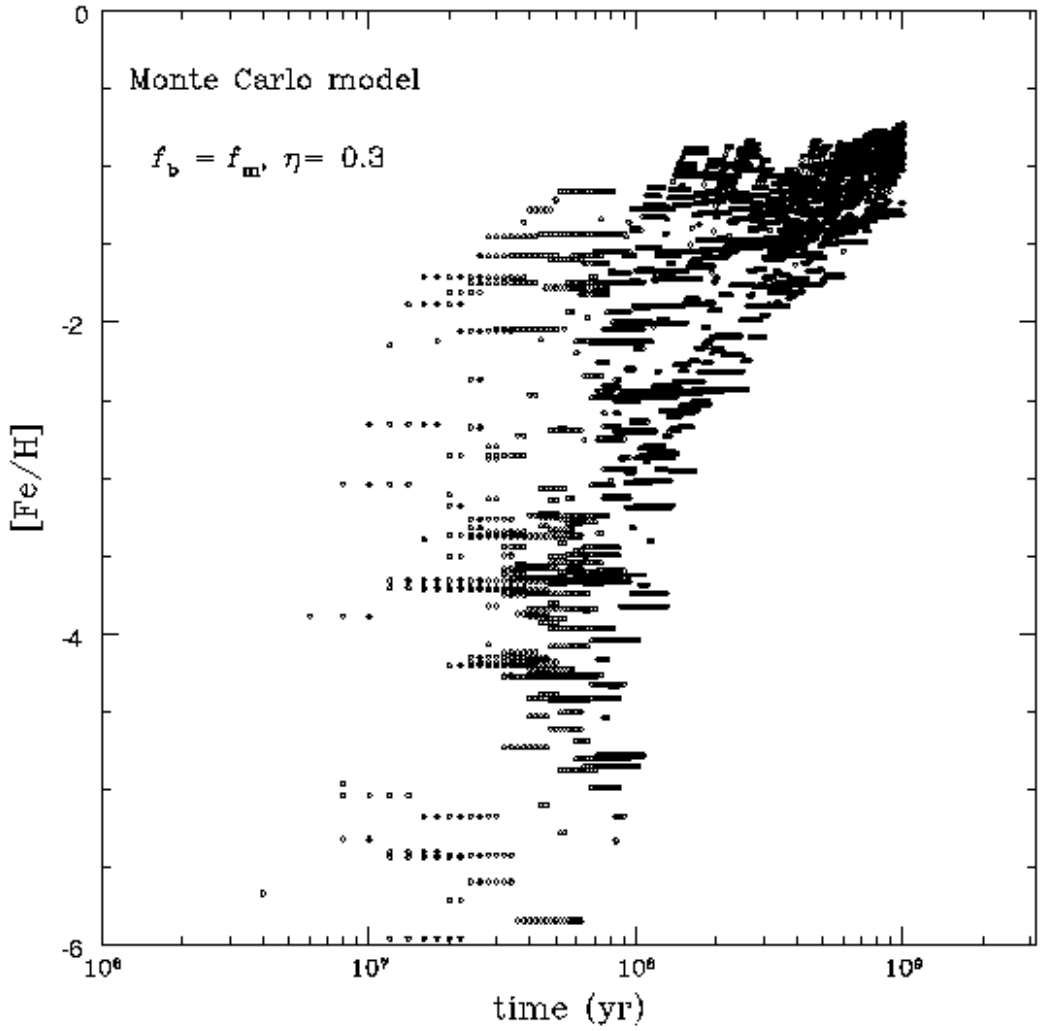

Fig. 6.— Distribution of metallicity vs. time obtained with the Monte Carlo model for the choice of frequency of coalescence $f_{\rm m}$ equal to the frequency of star formation $f_{\rm b}$, and with efficiency $\eta = 0.3$

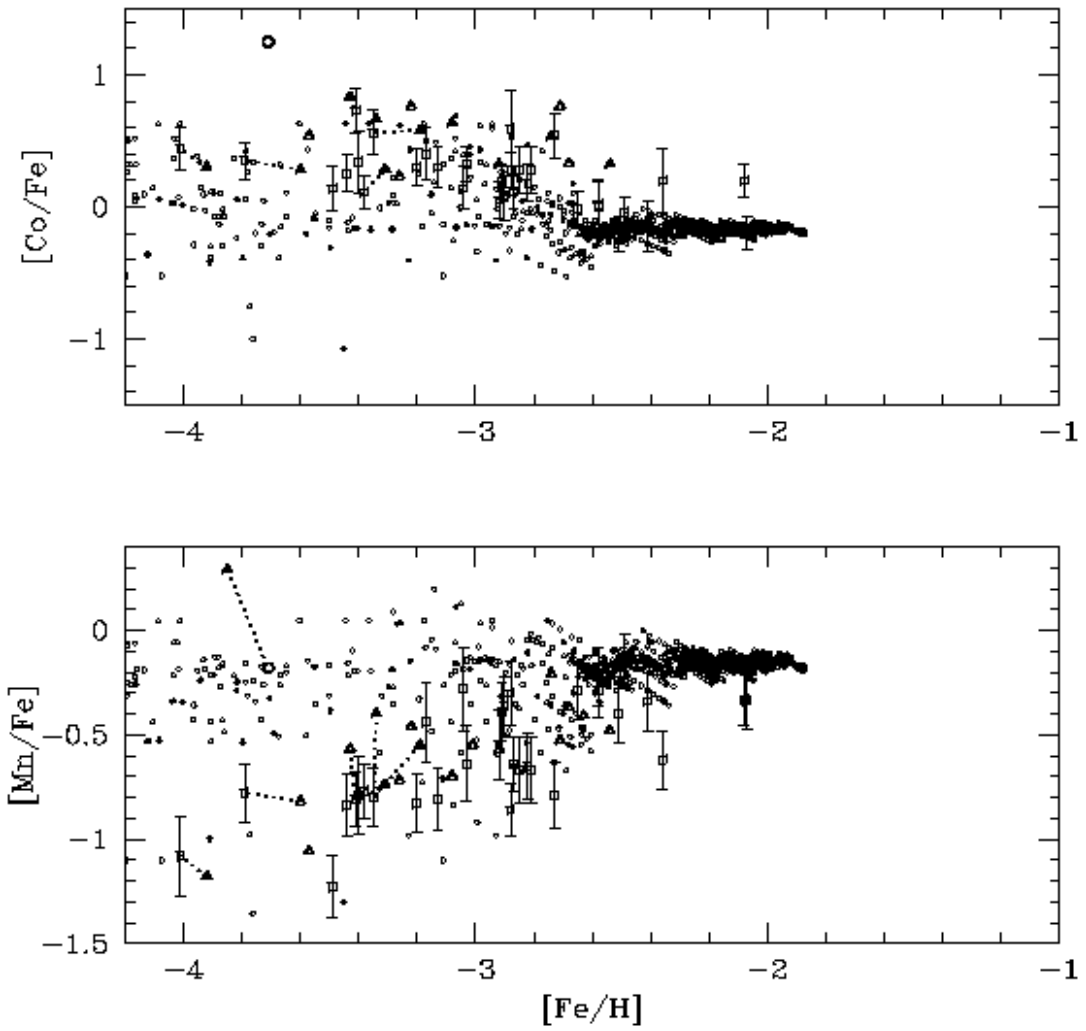

Fig. 7.— Enrichment of Co (*upper panel*) and Mn (*lower panel*) in the halo gas at different metallicities. Small open circles represent interstellar clouds in the Monte Carlo model. Observational data are from: McWilliam et al. (1995b) (*open squares*), Ryan et al. (1996) (*open triangles*), and Norris et al. (2000) (*open circles*). Thin dotted lines connect same stars with different abundance determinations. Errorbars are shown only when reported by the authors for single objects.

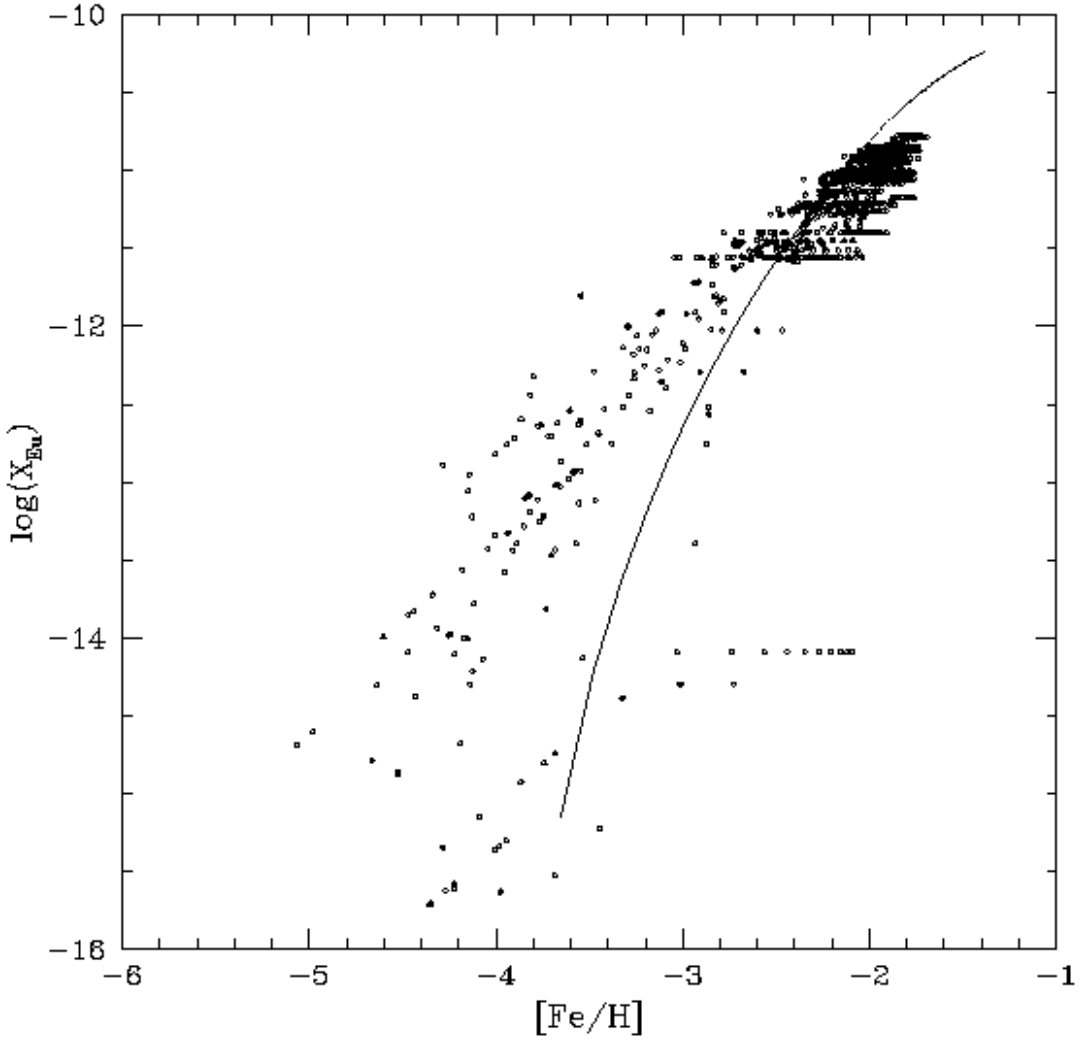

Fig. 8.— Enrichment of Eu in the halo gas at different metallicities during the first Gyr of Galactic evolution. Small open circles represent interstellar clouds in the Monte Carlo model. The *solid line* represents the one-zone halo model presented in Travaglio et al. (1999).

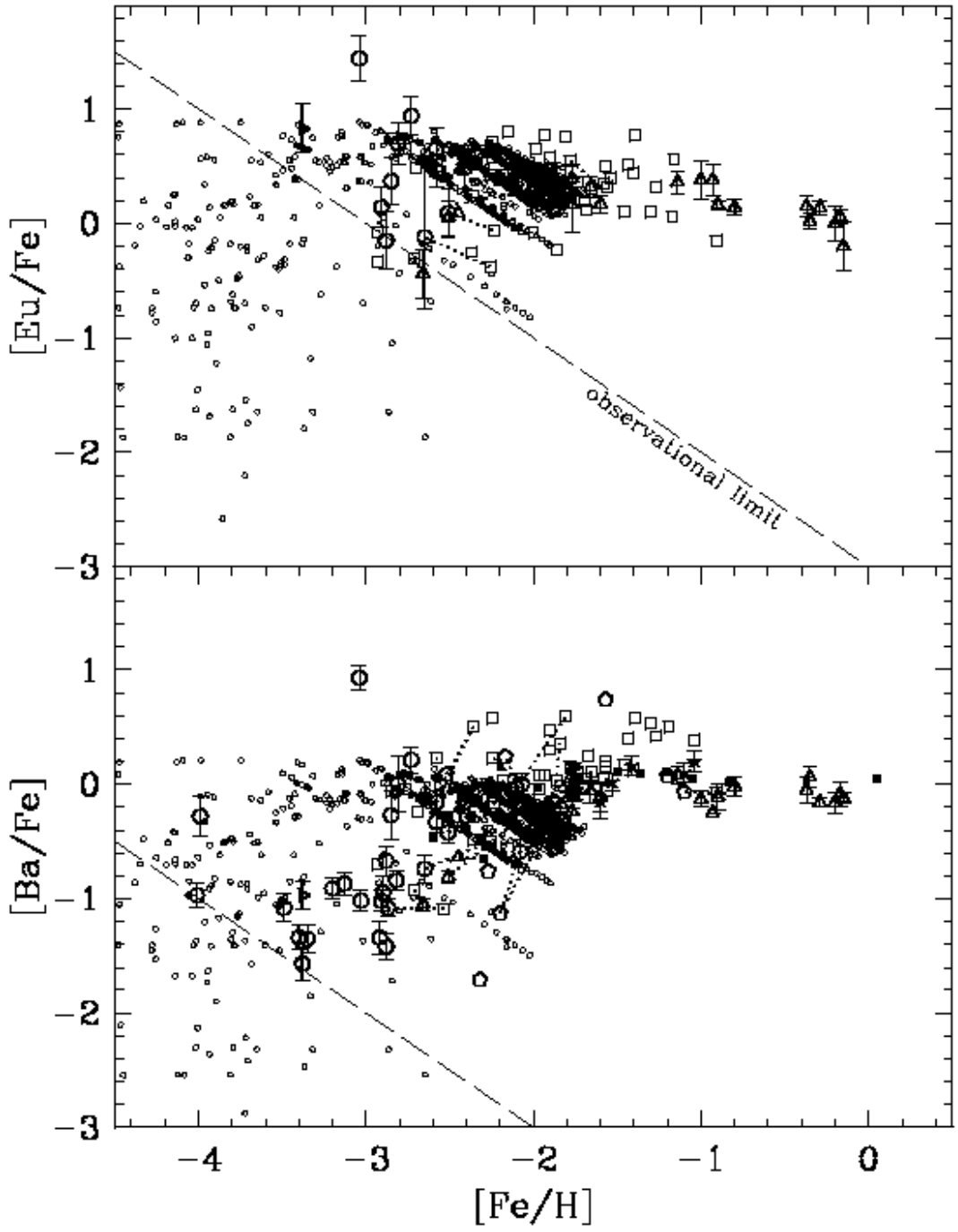

Fig. 9.— Abundance of Eu (*upper panel*) and Ba (*lower panel*), as a function of [Fe/H], during the first Gyr of evolution of the Galaxy (model predictions are shown as *small thin open circles* and represent our best-fit model with the choice parameters reported in Table 1). The *long-dashed line* indicates the sensitivity limit for observing Eu and Ba. The *r*-process yields of Eu are derived from SNII in the mass range 8–10 $M_{\odot}$. Observational data of Eu and Ba in metal-poor stars are from: Gratton & Sneden (1994) (*open triangles*); Woolf et al. (1995) (*open squares*); François (1996) (*pentagons*); McWilliam et al. (1995) and McWilliam (1998) (*thick open circles*); Norris, Ryan & Beers (1997) (*open tilted triangles*); Jehin et al. (1998) (*filled tilted triangles*); Mashonkina et al. 1999 (*filled squares*); Burris et al. (2000) (*open squares*). Thin dotted lines

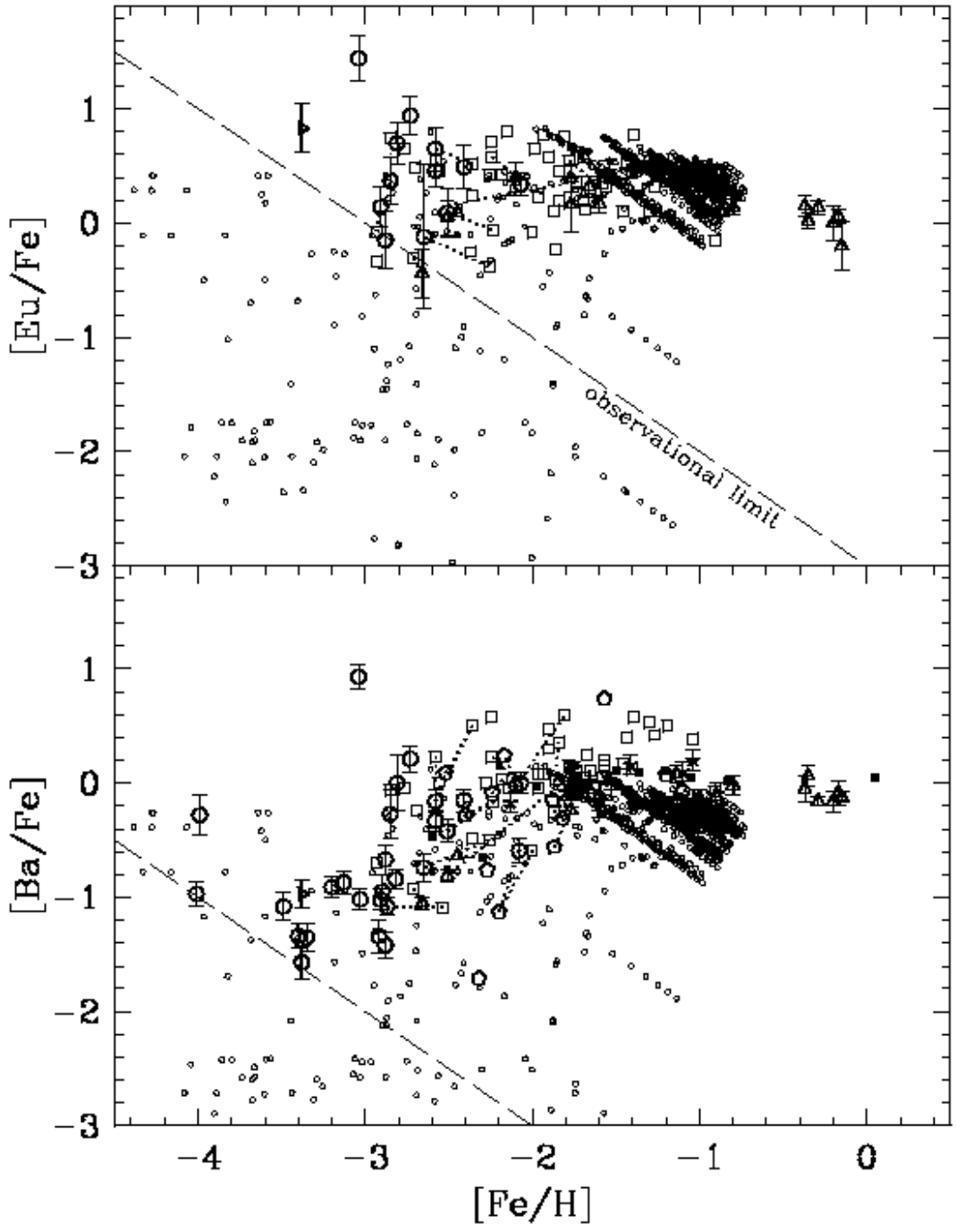

Fig. 10.— The same of Fig. 10, for star formation efficiency $\eta = 0.3$ (see text for discussion)

.

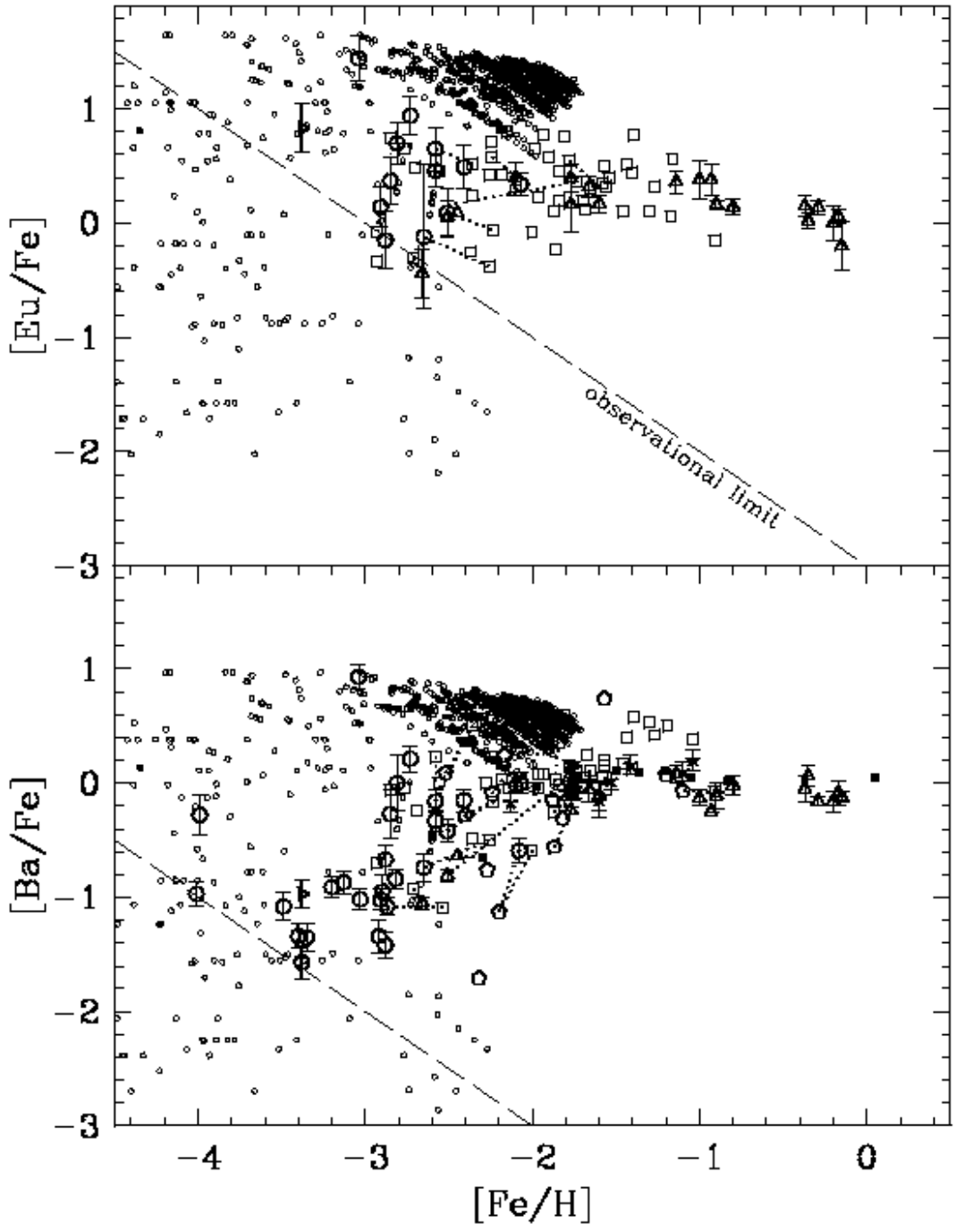

Fig. 11.— The same of Fig. 9, in which Eu and Ba are produced by SNII in the mass range 15–30 $M_{\odot}$.

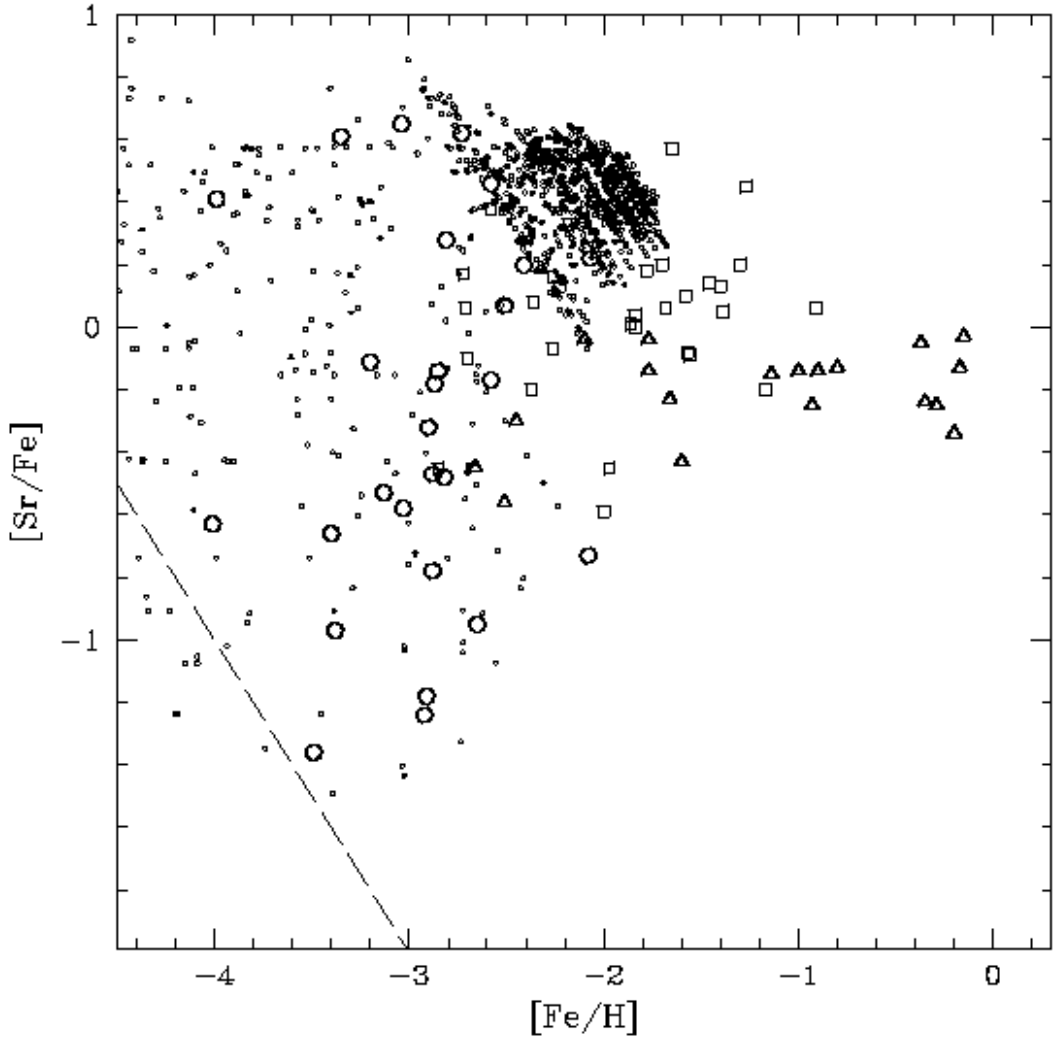

Fig. 12.— Chemical evolution of Sr, under the assumption described in the text, and with an additional primary component from SNII with masses $\sim$ 15–25 $M_{\odot}$, accounting for $\sim$ 20% of the solar Sr abundance. The Monte Carlo model results are shown as *small thin open circles*. Observational data are from: Burris et al. (2000) (*open squares*); McWilliam (1998) (*open circles*); Gratton & Sneden (1994) (*open triangles*). The *long-dashed line* indicates the sensitivity limit for observing Sr.